

# Cosmic Rays

## 1. Introduction

Lecture 1: Introduction to cosmic rays

Lecture 2: Atmospheric  $\mu$  and  $\nu$  and  $\nu$  telescopes

Lecture 3: Giant air shower experiments

Exercise: Expectations for  $\gamma$ -ray &  $\nu$ -astronomy

# Highlights of history of cosmic rays

- 1912: Victor Hess, Nobel prize 1936
  - Ascended to 5300 m in an open balloon
  - Showed ionization of the air increased
- ~1920: Millikan (Caltech)
  - coined “cosmic rays”
  - thought they were photons
  - Compton (at Chicago) argued they were positive particles
- 1930's: latitude surveys, Geiger counters
  - E-W effect proves primary cosmic rays are +charged
  - Atmospheric secondaries are muons, photons and  $e^\pm$
- 1940's: (post-war) photographic emulsions
  - 1947 Powell et al., discovery of the pion
  - 1948 discovery of nuclei in primary cosmic radiation
  - 1949 Fermi (Chicago) paper on cosmic-ray acceleration

# Air shower history

- 1937: Pierre Auger discovery
  - Observed earlier by Rossi
- 1940's: Rossi (M.I.T.)
  - Air shower studies with arrays of scintillators
- 1960's: discovery of the “knee”
  - Bernard Peters points out need for a new population
  - 1962: John Linsley (Volcano Ranch)
    - "[Evidence for a Primary Cosmic-Ray Particle with Energy  \$10^{20}\$  eV](#)". *Physical Review Letters* **10**: 146, 1963
- AGASA, Fly's Eye, HiRes, Auger, TA ...

# Tibet hybrid air shower array

4300 m  $\sim 600 \text{ g/cm}^2$



An aerial photograph of an Antarctic research station, identified as IceTop. The station is situated on a vast, flat, snow-covered landscape. Numerous buildings, tents, and other structures are scattered across the site, with a central cluster of larger buildings. A network of tracks, likely from vehicles or sleds, crisscrosses the snowfield. In the upper left, a large, dark, dome-like structure is visible. The sky is overcast and grey. The text "IceTop" is printed in the upper right corner. A scale bar with arrows at both ends and the text "125 m" is located in the lower left quadrant. The photo credit "Photo by James Roth 17 December 2007" is in the lower right corner.

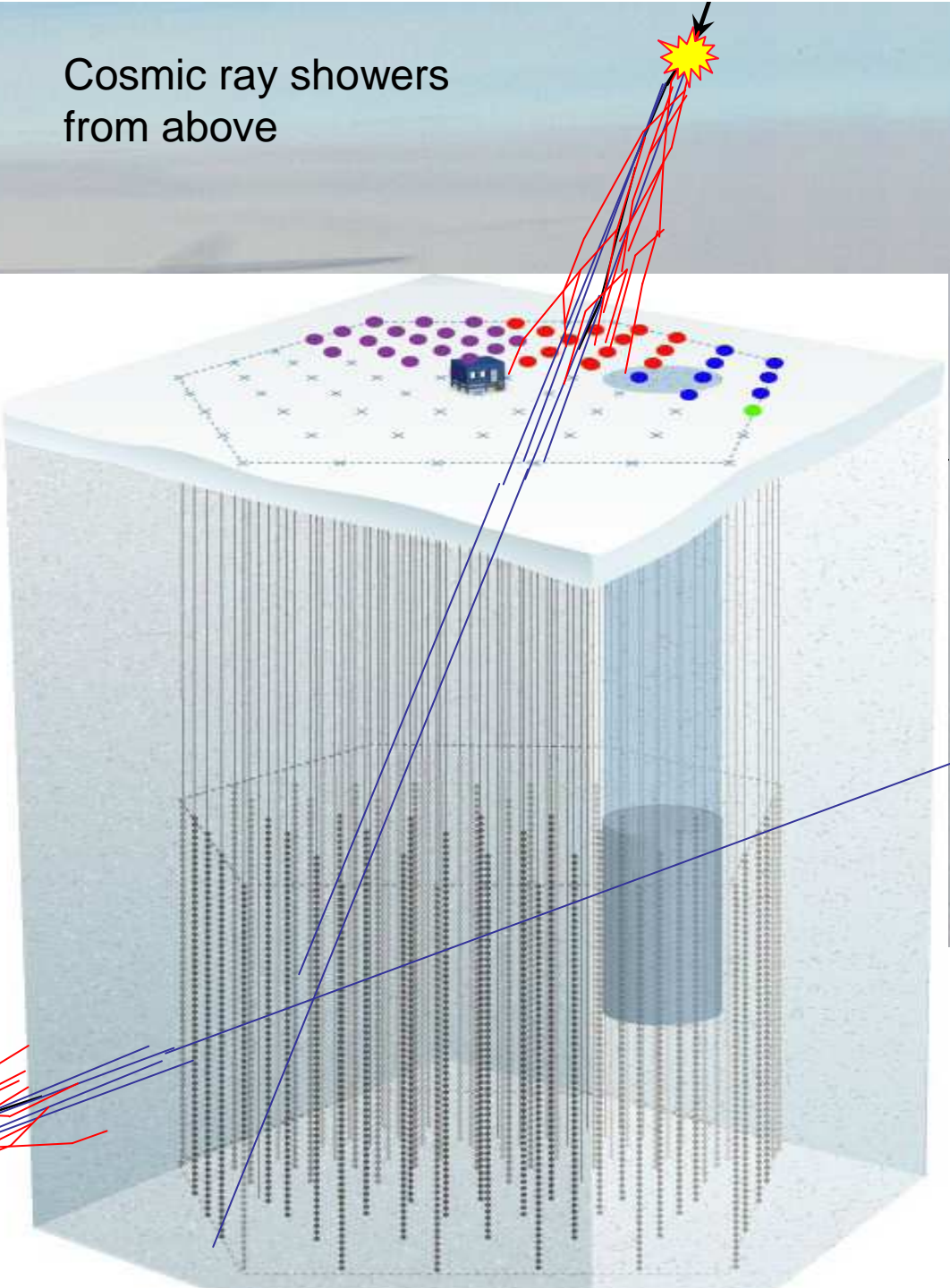
IceTop

125 m

Photo by James Roth  
17 December 2007



Cosmic ray showers  
from above



Neutrinos from all directions

Berlin, 2009 29 Sept

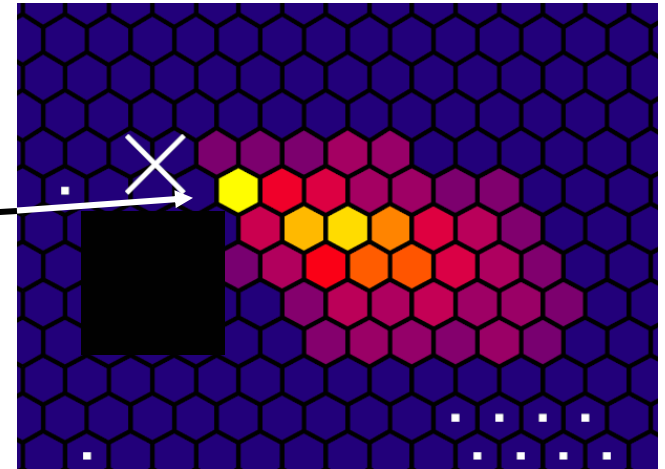
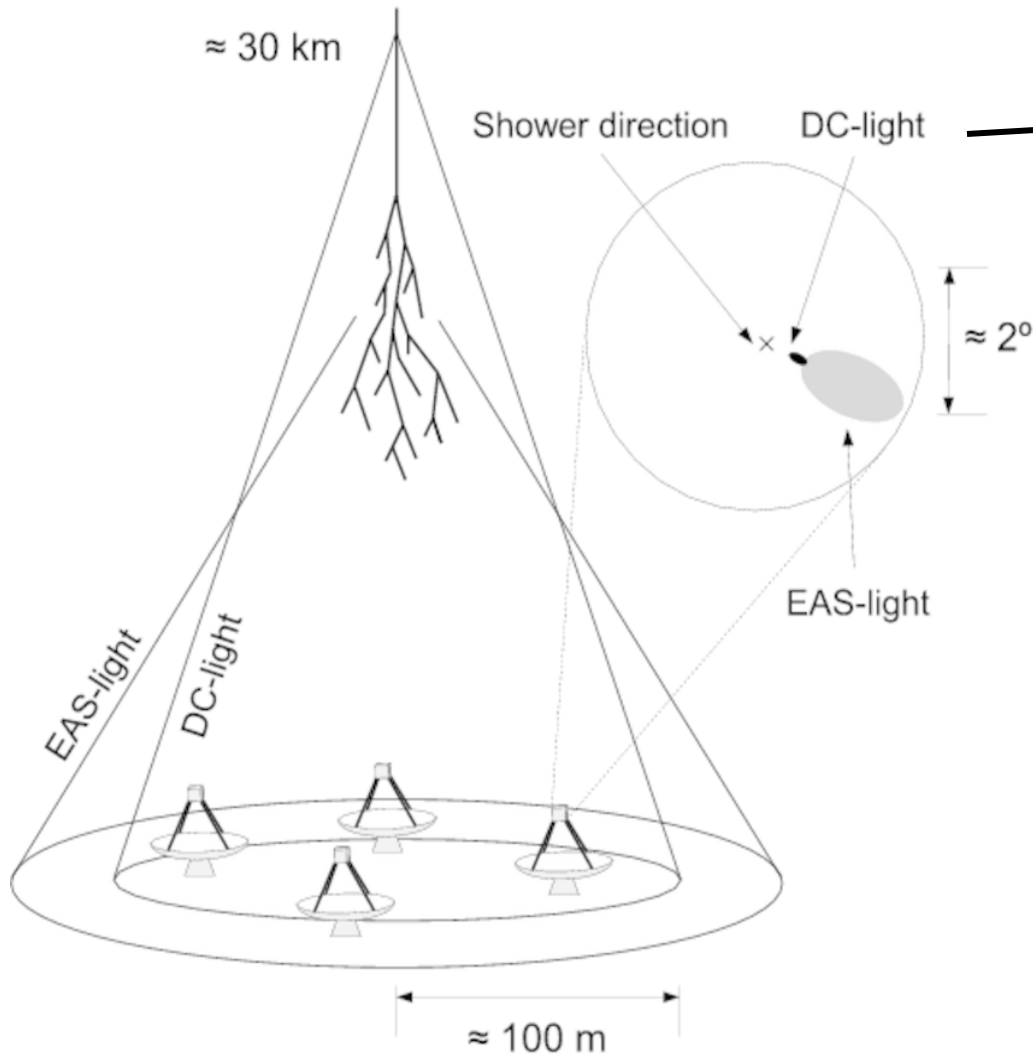


# $\gamma$ -ray telescopes

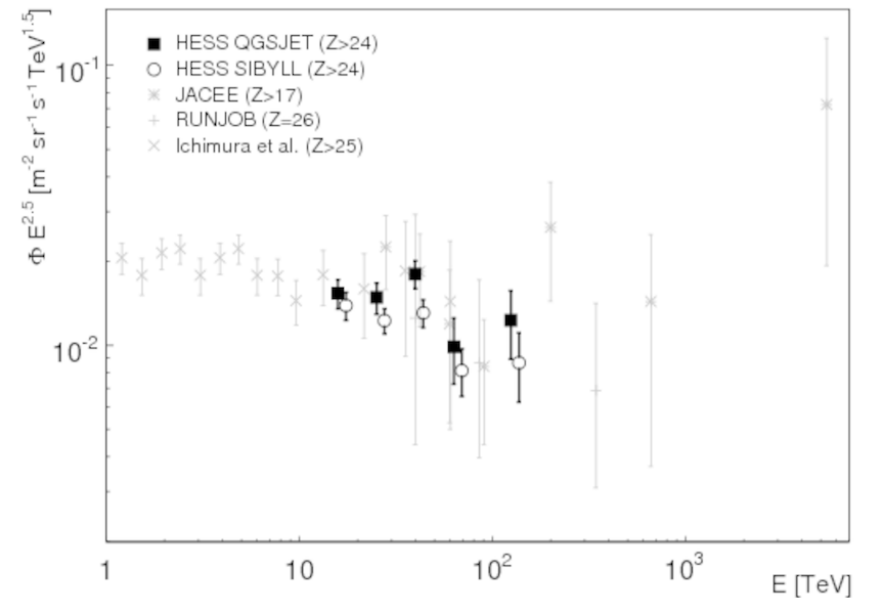


# CR Iron spectrum from Direct Cherenkov

HESS collaboration, Phys Rev D 27, 2007

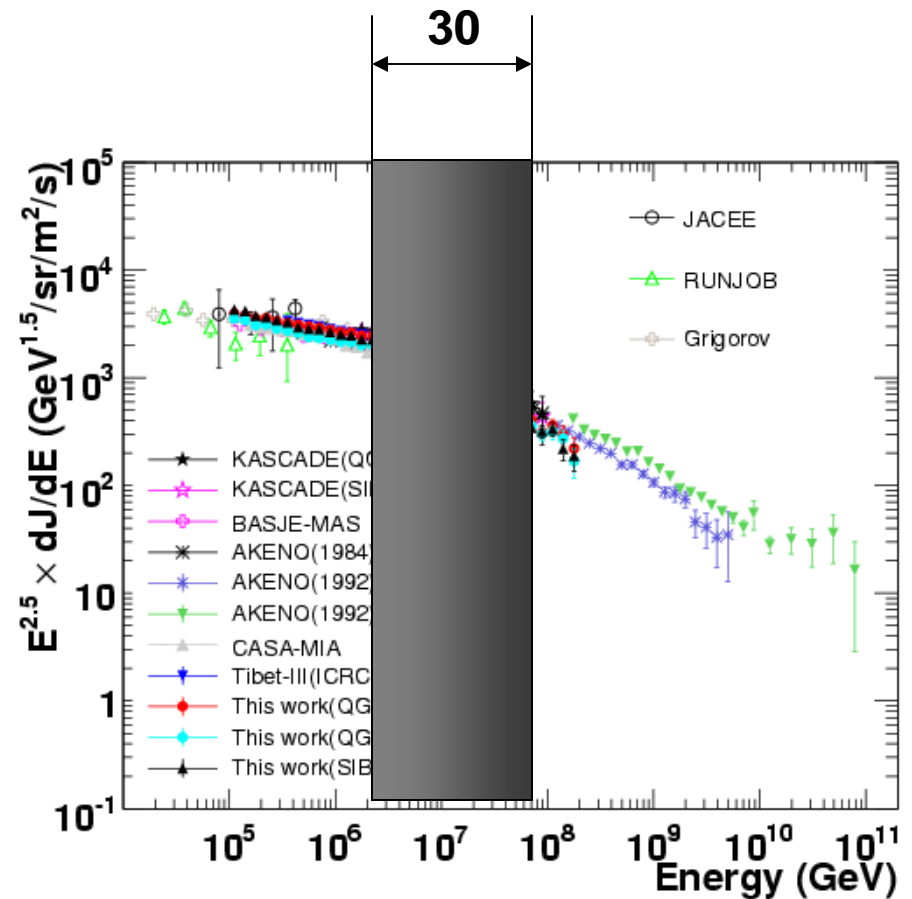


Method proposed by Kieda et al, 2001



# Rigidity-dependence

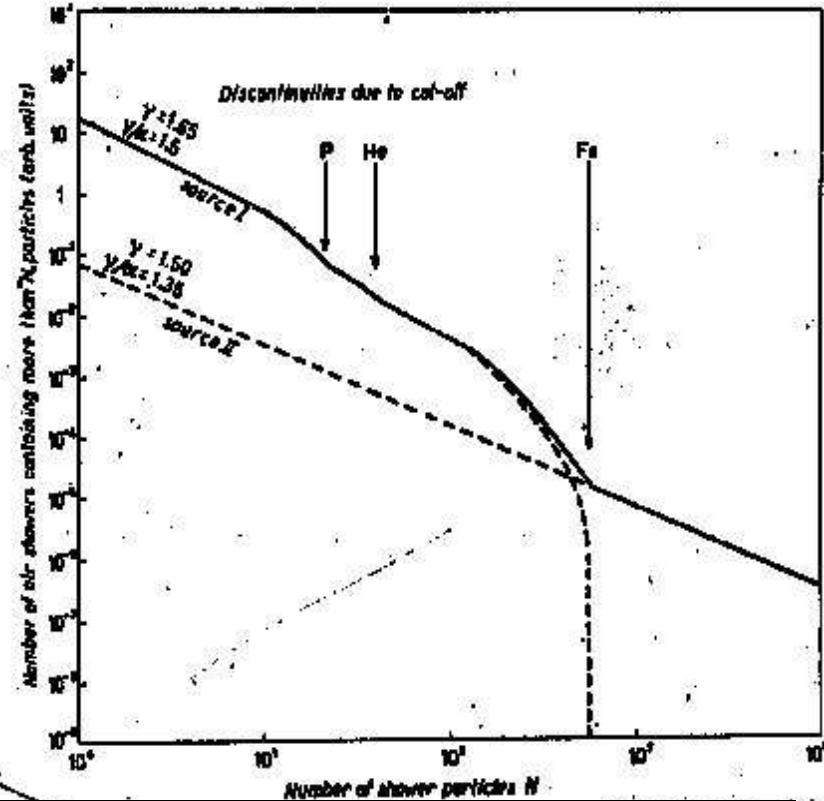
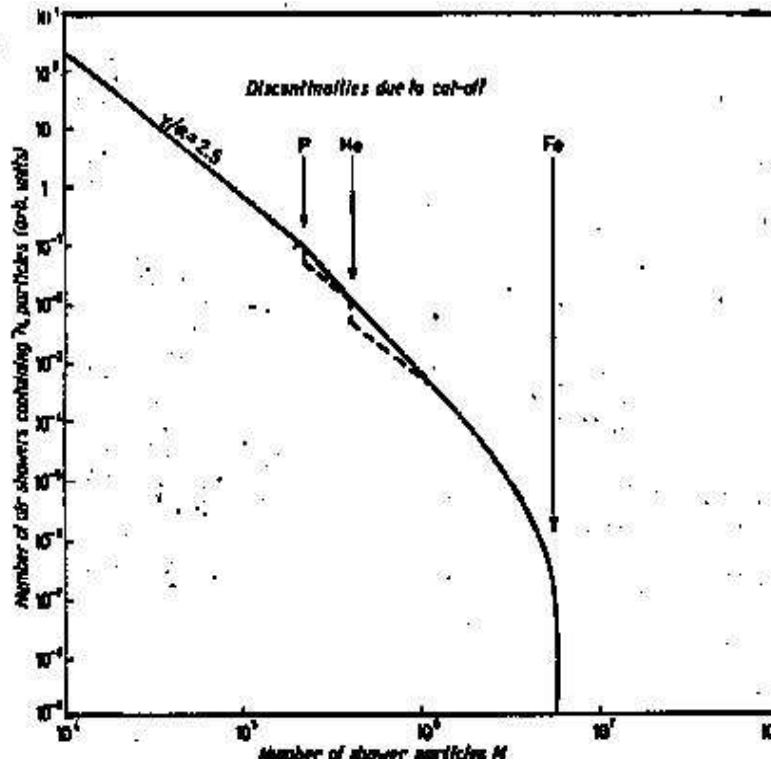
- Acceleration, propagation
  - depend on B:  $r_{\text{gyro}} = R/B$
  - Rigidity,  $R = E/Zc$
  - $E_c(Z) \sim Z R_c$
- $r_{\text{SNR}} \sim \text{parsec}$ 
  - $\rightarrow E_{\text{max}} \sim Z * 10^{15} \text{ eV}$
  - $1 \leq Z \leq 30$  (p to Fe)
- Slope change should occur within factor of 30 in energy
- With characteristic pattern of increasing A
- Problem: continuation of smooth spectrum to EeV
- More on this later...



# B. Peters: if $E_{\max}$ depends on B then p disappear first, then He, C, O, etc.

Peters cycle: systematic increase of  $\langle A \rangle$  approaching  $E_{\max}$

$\langle A \rangle$  should begin to decrease again for  $E > 30 \times E_{\text{knee}}$



$$\text{gyro-radius} = Pc / ZeB \equiv R \text{ (rigidity)} / B$$

$$\Rightarrow E_{\text{knee}} \sim Z \times R(\text{knee})$$

Tom Ga

B. Peters, Nuovo Cimento 22 (1961) 800

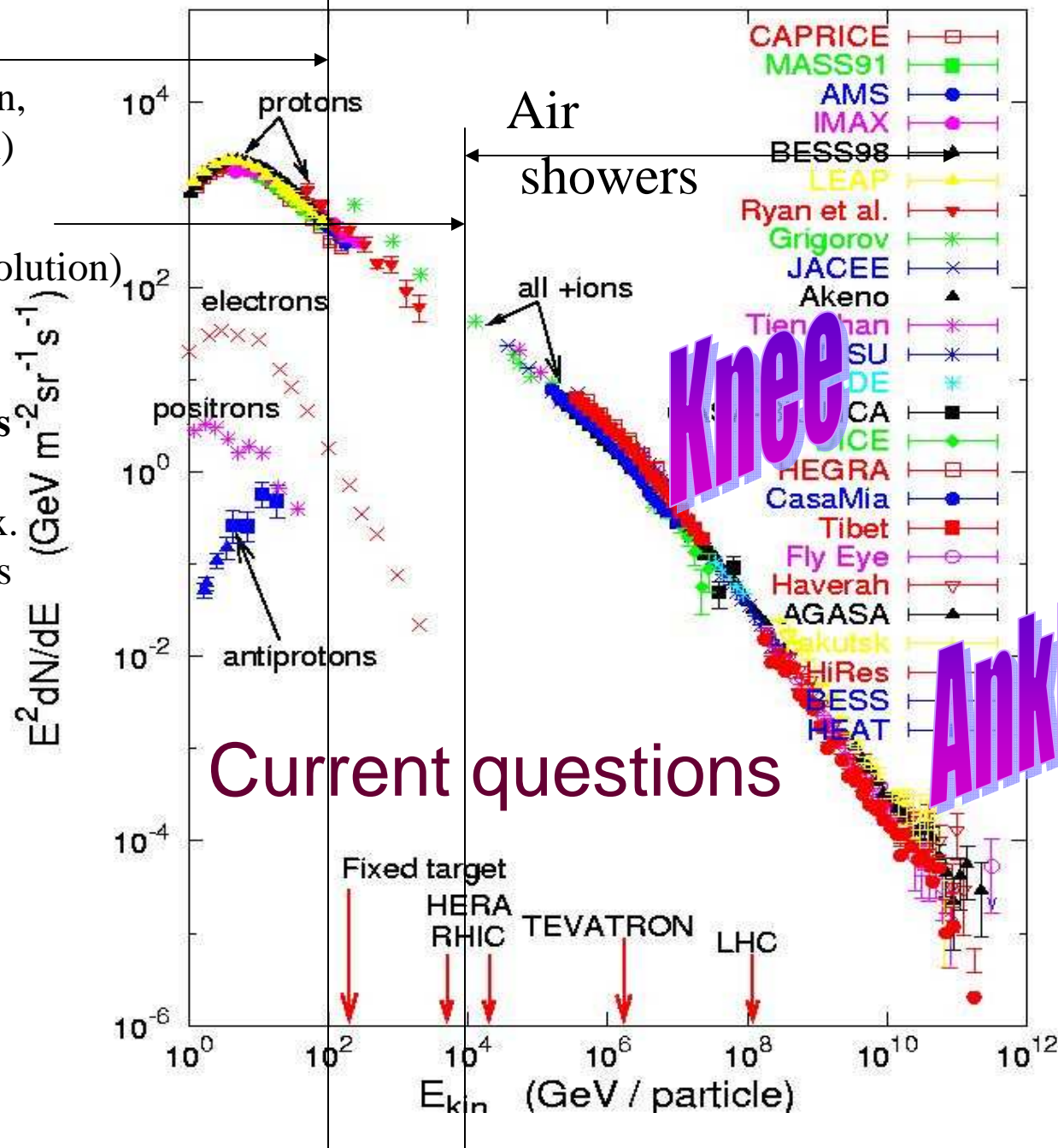
# Primary spectrum

Energies and rates of the cosmic-ray particles

**Spectrometers**  
 ( $\Delta A = 1$  resolution,  
 good E resolution)

**Calorimeters**  
 (less good resolution)

**Air-shower arrays**  
 on the ground to  
 overcome low flux.  
 Don't see primaries  
 directly.



# 31<sup>st</sup> Int. Cosmic Ray Conf.

July 7-15, 2009, Łódź, Poland

## *Scientific program*

### **Solar and Heliospheric**

SH.1: SOLAR EMISSIONS

SH.2: ACCELERATION AND PROPAGATION IN THE HELIOSPHERE

SH.3: GALACTIC COSMIC RAYS IN THE HELIOSPHERE

### **Origin and Galactic**

OG.1: LOW ENERGY COSMIC RAYS

OG.2: X-RAY, GAMMA-RAY AND NEUTRINO ASTRONOMY AND ASTROPHYSICS

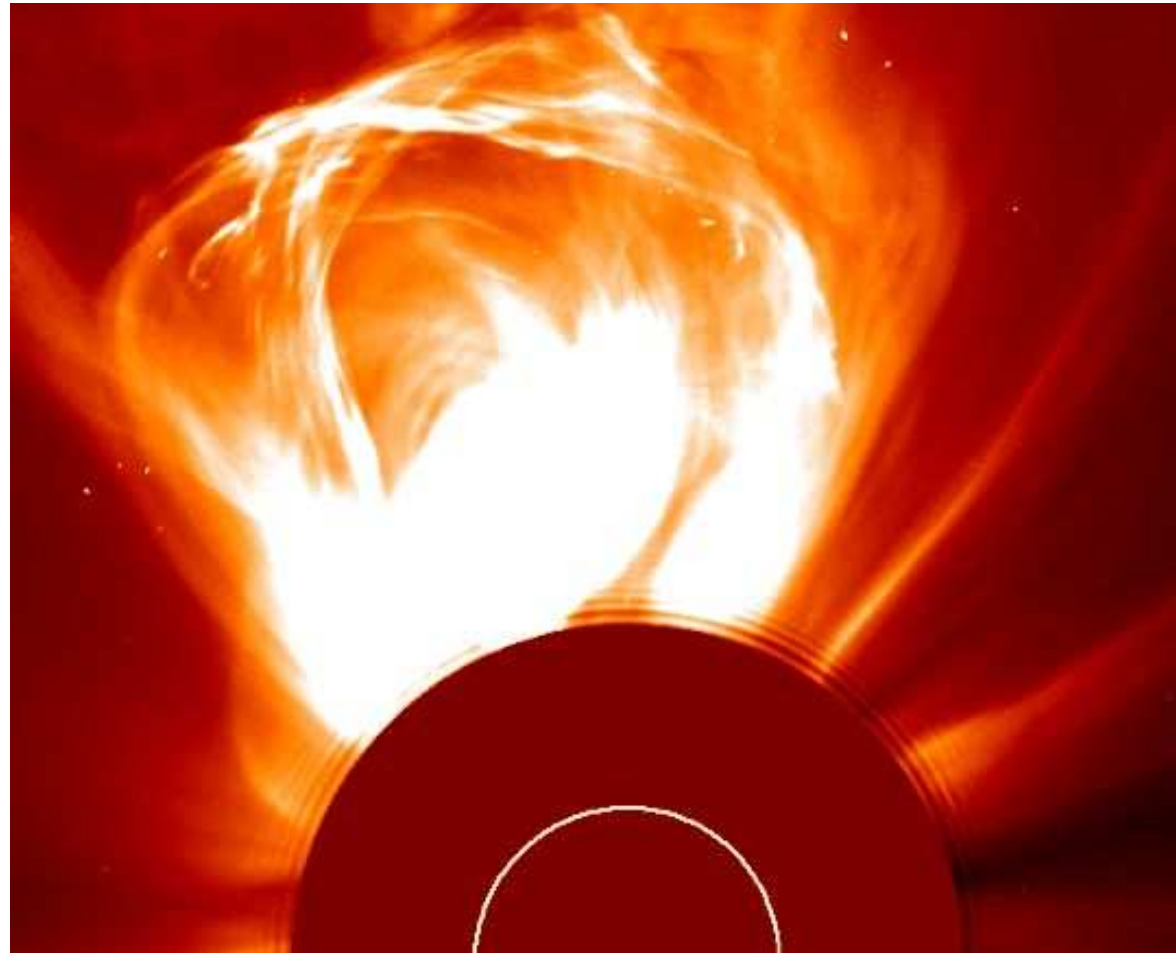
### **High Energy**

HE.1: HIGH ENERGY COSMIC RAYS – EAS

HE.2: PARTICLE PHYSICS, ASTRO-PARTICLE PHYSICS AND COSMOLOGY

# Solar flare shock acceleration

Coronal mass ejection  
09 Mar 2000

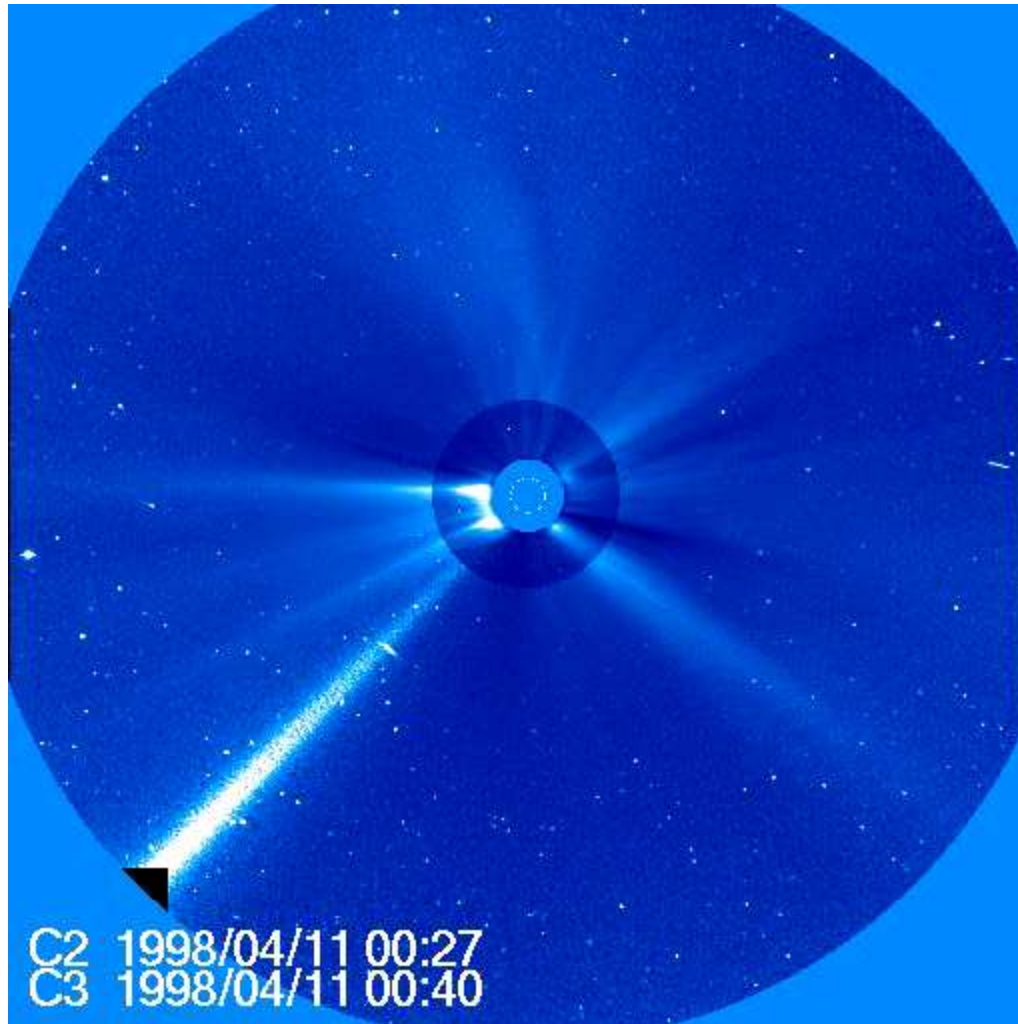


Berlin, 2009 29 Sept

Tom Gaisser

13

# Movie: LASCO on SOHO

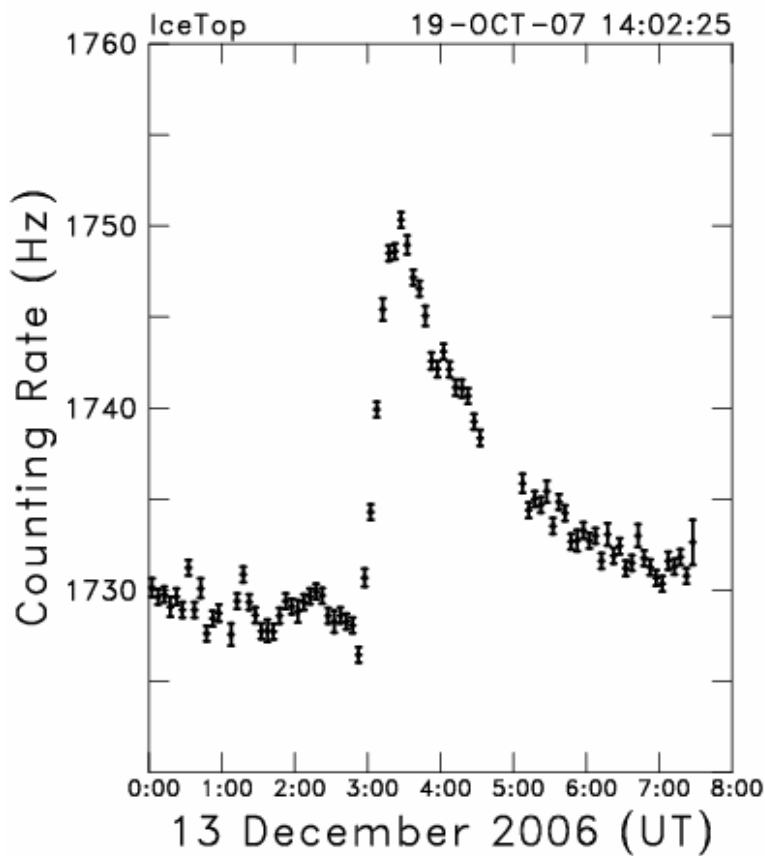


# Movie from LASCO instrument on SOHO

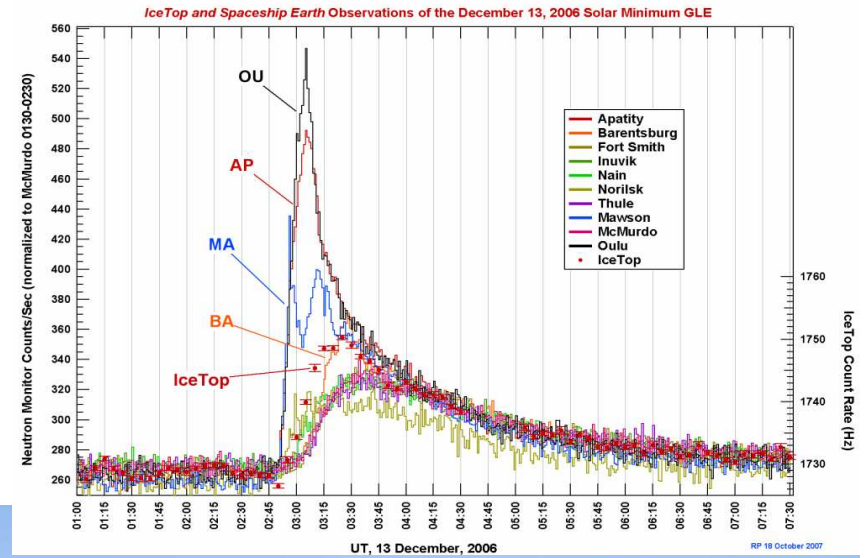
**1998 April 11 - 20: An interesting period:  
Between April 10 and April 13, a comet enters the field of view from the left (East) and passes around the Sun.  
On April 10-11, a smaller sun-grazing comet approaches the Sun from the south, just to the right of the occulter pylon.  
The period culminates in a fast CME associated with a high energy particle storm at SOHO**

# 13 Dec 2006 solar flare: GLE in IceTop

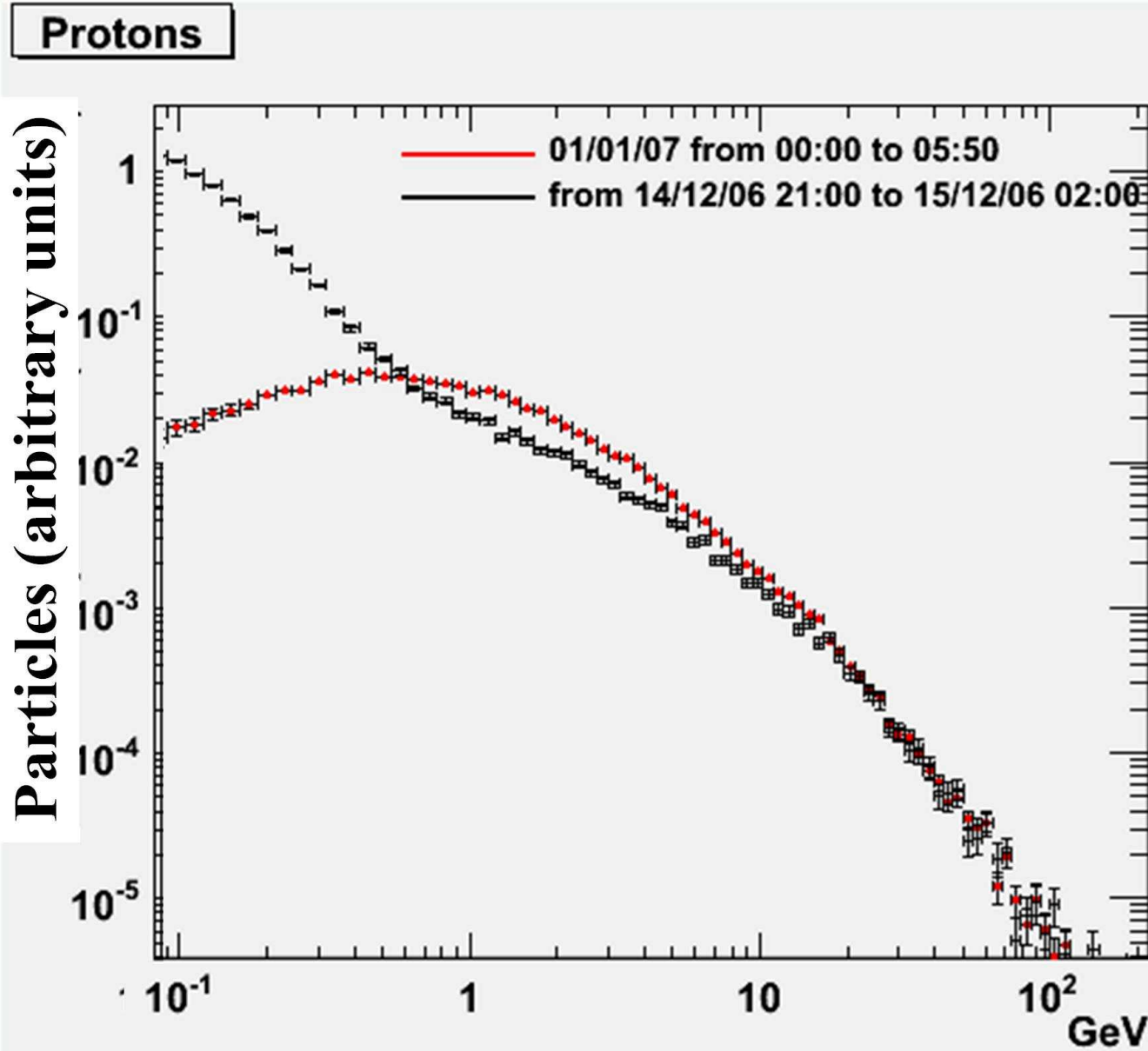
With 32 tanks in 2006



Ap. J. (Letters) 689 (2008) L65-L68

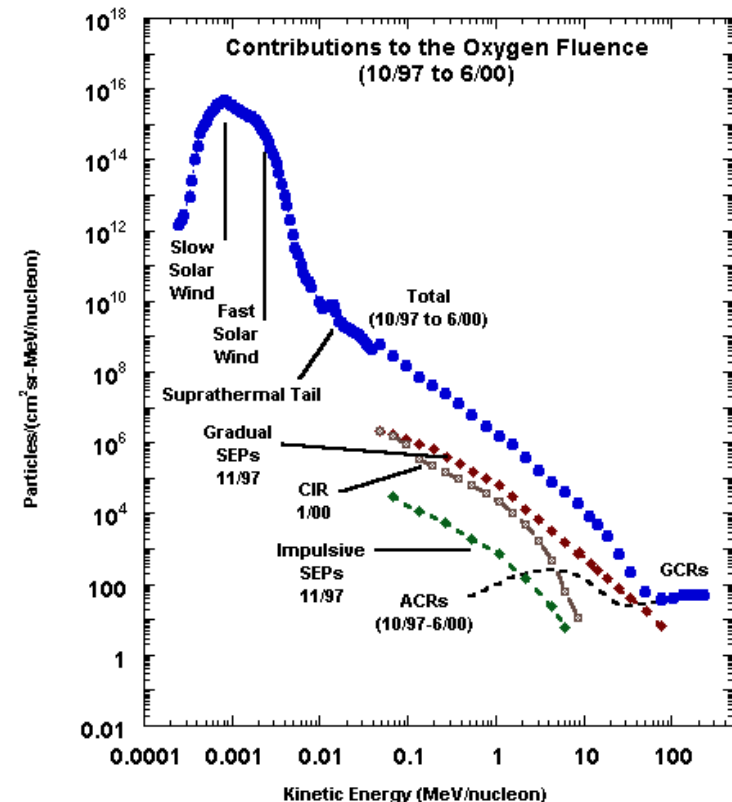


# Solar flare



# Lessons from the heliosphere

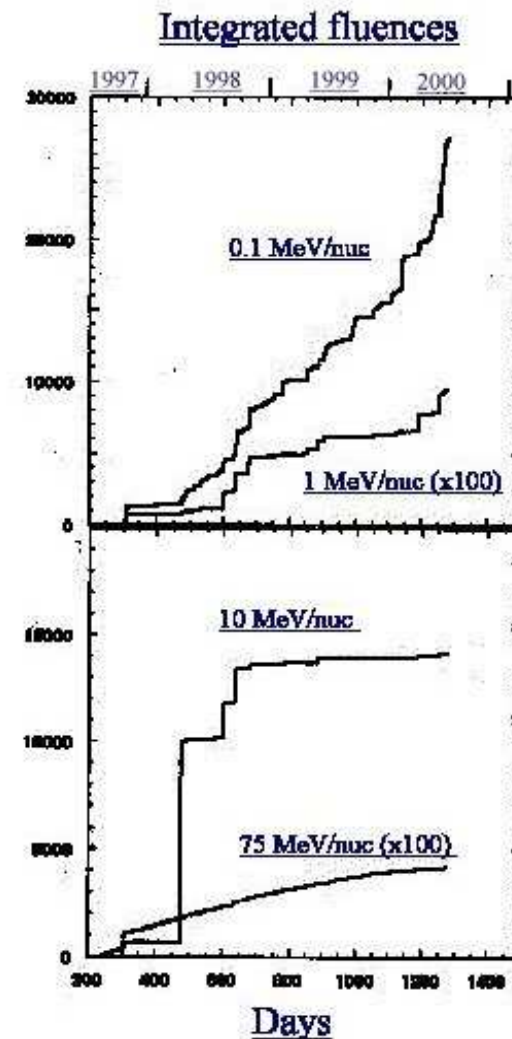
- ACE energetic particle fluences:
- Smooth spectrum
  - composed of several distinct components:
    - Most shock accelerated
    - Many events with different shapes contribute at low energy ( $< 1$  MeV)
    - Few events produce  $\sim 10$  MeV
  - Knee  $\sim E_{\text{max}}$  of a few events
  - Ankle at transition from heliospheric to galactic cosmic rays



**R.A. Mewaldt** *et al.*, A.I.P. Conf. Proc. 598 (2001) 165

# Heliospheric cosmic rays

- ACE--Integrated fluences:
  - Many events contribute to low-energy heliospheric cosmic rays;
  - fewer as energy increases.
  - Highest energy (75 MeV/nuc) is dominated by low-energy *galactic* cosmic rays, and this component is again *smooth*



**R.A. Mewaldt** *et al.*, A.I.P. Conf. Proc. 598 (2001) 165

# Galactic cosmic rays

Measurements from TRACER, BESS and others

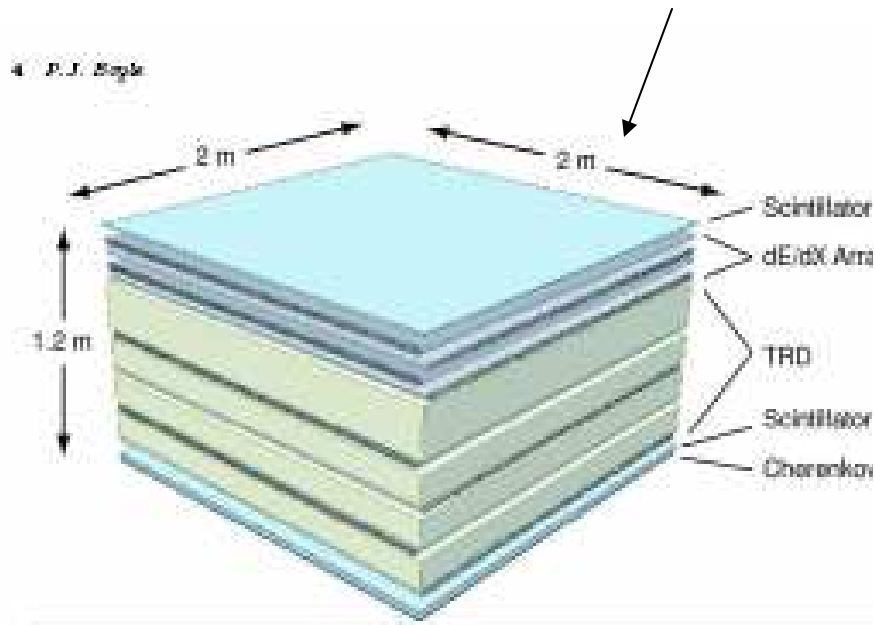


Fig. 2. Schematic diagram of the TRACER detector as flown during the Antarctic balloon mission in 2002. (From Aue et al.)

The Elemental Composition of High-Energy Cosmic Rays: Measurements with TRACER 5

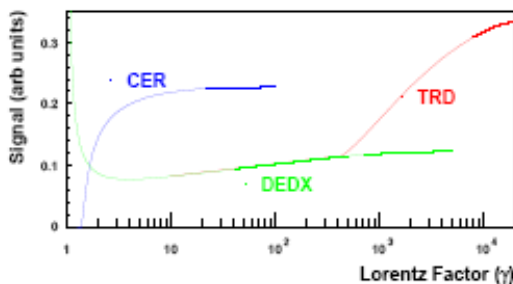


Fig. 3. Energy scale of TRACER. TRACER contains three energy measurements to cover more than 4 decades in energy. The relative amplitude of the response curves is representative of the signal/ $\beta^2$  in each detector (From Aue et al.)

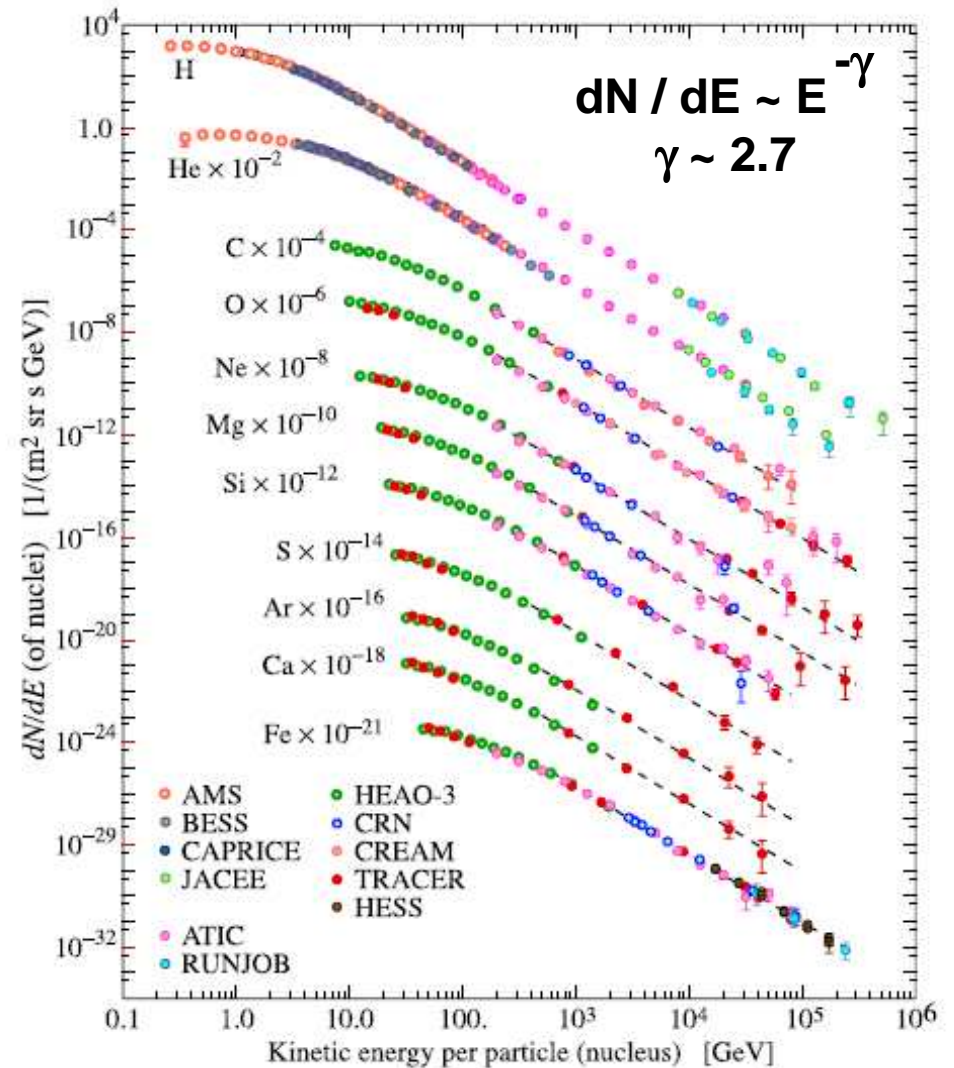
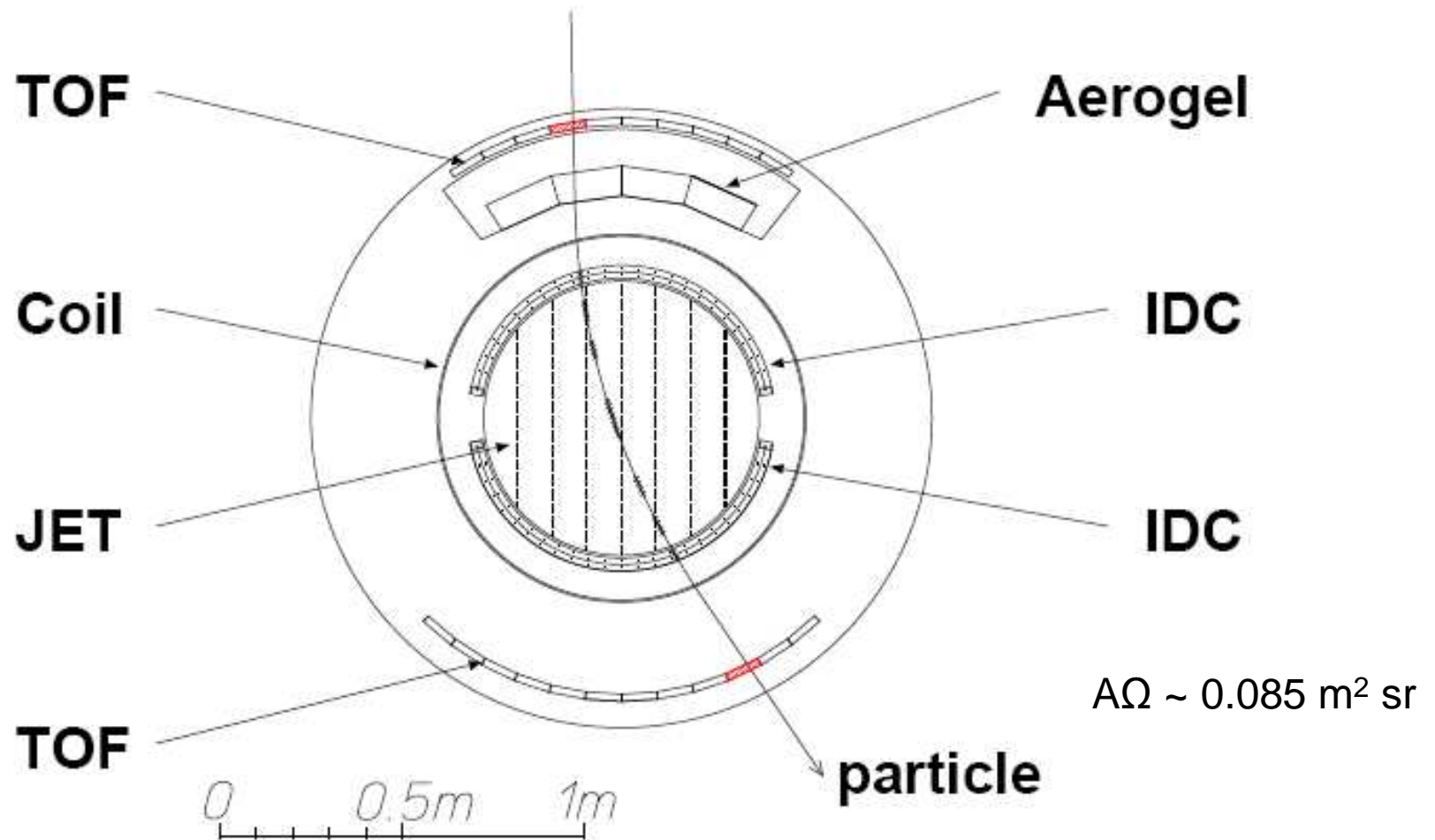


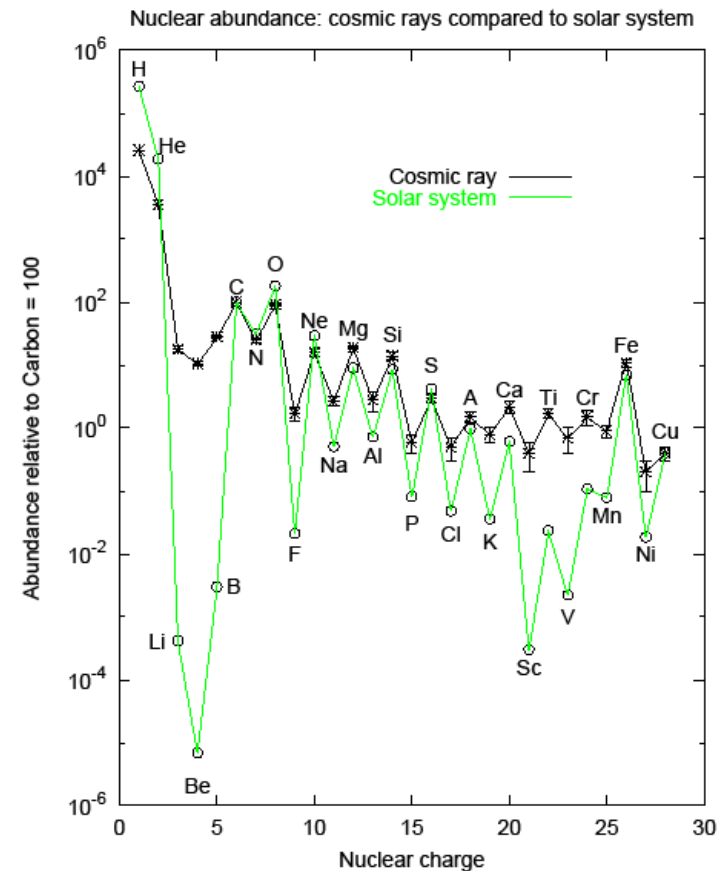
Figure by P. Boyle & D. Müller in RPP

# BESS spectrometer



# A fundamental result

- Excess of Li, Be, B from fragmentation of C, O
- Spallation  $\sigma$  plus  $\rho_{\text{ISM}}$  give dwell time of nuclei
  - Find  $\tau \sim 3 \times 10^6$  yrs
  - $c\tau \sim \text{Mpc} \gg$  size of galactic disk (kpc)
  - Suggests diffusion in turbulent ISM plasma
  - Predictions for  $\gamma$ -rays, positrons and antiprotons follow



# Energy-dependence of secondary/primary cosmic-ray nuclei

- $B/C \sim E^{-0.6}$
- Observed spectrum:
  - $\phi(E) = dN/dE \sim K E^{-2.7}$
- Interpretation:
  - Propagation depends on  $E$
  - $\tau(E) \sim E^{-0.6}$
  - $\phi(E) \sim Q(E) \times \tau(E) \times (c/4\pi)$
- Implication:
  - Source spectrum:

$$Q(E) \sim E^{-2.1}$$

Berlin, 2009 29 Sept

Tom Gaisser

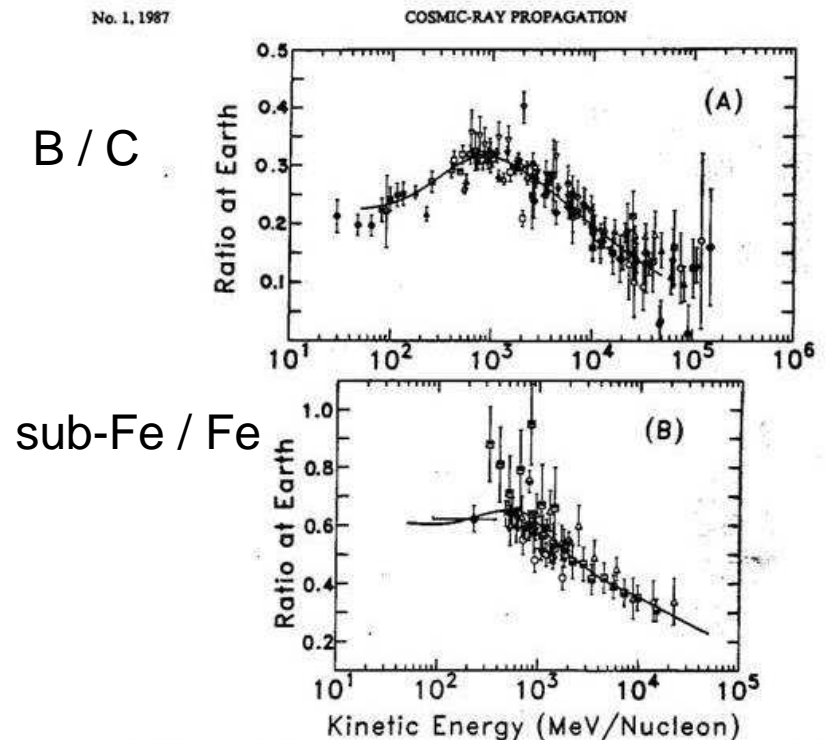


FIG. 10.—The ratios (a) B/C and (b) sub-Fe/Fe of Fig. 3 compared with the results of a propagation calculation using a path-length  $\lambda$  includes an energy-dependent deficiency of short path lengths as well as an energy-dependent mean for the exponential part of the distri for details.)

Garcia-Munoz, Simpson, Guzik, Wefel  
& Margolis, Ap. J. 64 (1987) 269 23

# Secondary / primary ratios from CREAM

arXiv: 0808.1718

- B is entirely secondary
- Source is production in ISM
- Spectral index at production is same as observed (propagated) primary nuclei
- Therefore observed spectral of B is  $2.7 + \delta = 2.1 + 2\delta \sim 3.3$

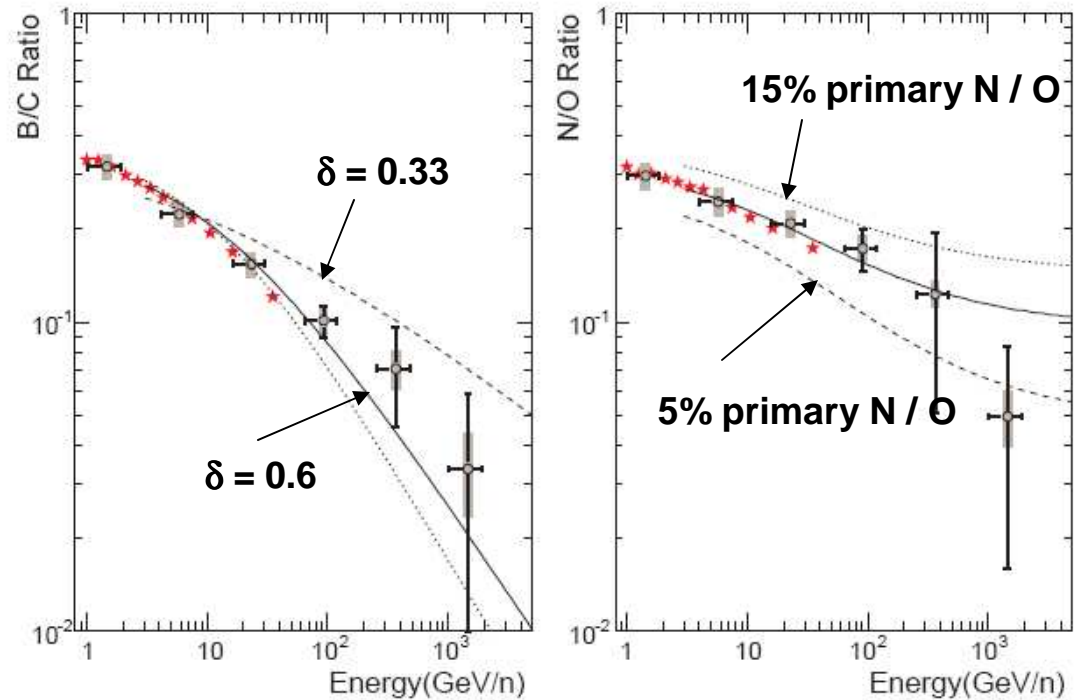


Fig. 7. Measurements of the ratios of nuclei as a function of energy. Left: Filled circles show the ratio of boron to carbon vs. energy after corrections. The horizontal errors are an estimate of the systematic error in the overall energy scale. The thin vertical lines correspond to the statistical error of the ratio and the grey bars show the systematic uncertainty in the ratio. See text for details. The lines represent model calculations for various values of the magnetic-rigidity dependence parameter,  $\delta$ , in escape from the Galaxy - as discussed in the text. These are; solid line  $\delta=0.6$ , long-dashed line  $\delta=0.333$ , short-dashed line  $\delta=0.7$ . The stars are data from the space experiment, HEAO-3-C2[5]. Right: Filled circles show the ratio of nitrogen to oxygen vs. energy after corrections. The error bars and data points are as in the left panel. The lines represent model calculations of this ratio with the escape parameter  $\delta=0.6$  (solid line in the top left-hand panel). The different curves correspond to different assumptions on the amount of nitrogen in the source material. These are; solid line source  $N/O = 10\%$ , long-dashed line source  $N/O = 5\%$ , short-dashed line  $N/O = 15\%$ .

# Energetics of cosmic rays

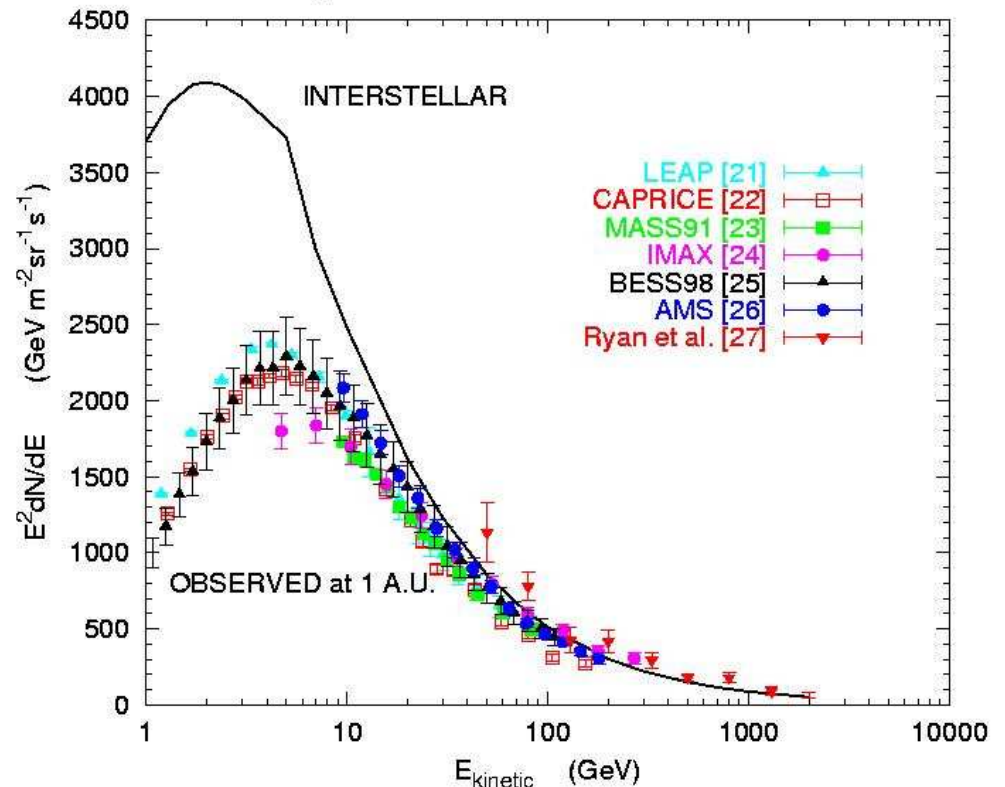
- Total local energy density:
  - $(4\pi/c) \int E\phi(E) dE$
  - $\sim 10^{-12} \text{ erg/cm}^3 \sim B^2 / 8\pi$
- Power needed:
  - $(4\pi/c) \int E\phi(E) / \tau_{\text{esc}}(E) dE$
  - galactic  $\tau_{\text{esc}} \sim 10^7 E^{-0.6} \text{ yrs}$
  - Power  $\sim 10^{-26} \text{ erg/cm}^3\text{s}$
- Supernova power:
  - $10^{51} \text{ erg per SN}$
  - $\sim 3 \text{ SN per century in disk}$
  - $\sim 10^{-25} \text{ erg/cm}^3\text{s}$
- SN model of galactic CR
  - Power spectrum from shock acceleration, propagation

## Spectral Energy Distribution

(linear plot shows most  $E < 100 \text{ GeV}$ )

$(4\pi/c) E\phi(E) = \text{local differential CR energy density}$

Energy Content of Galactic Cosmic-ray Protons

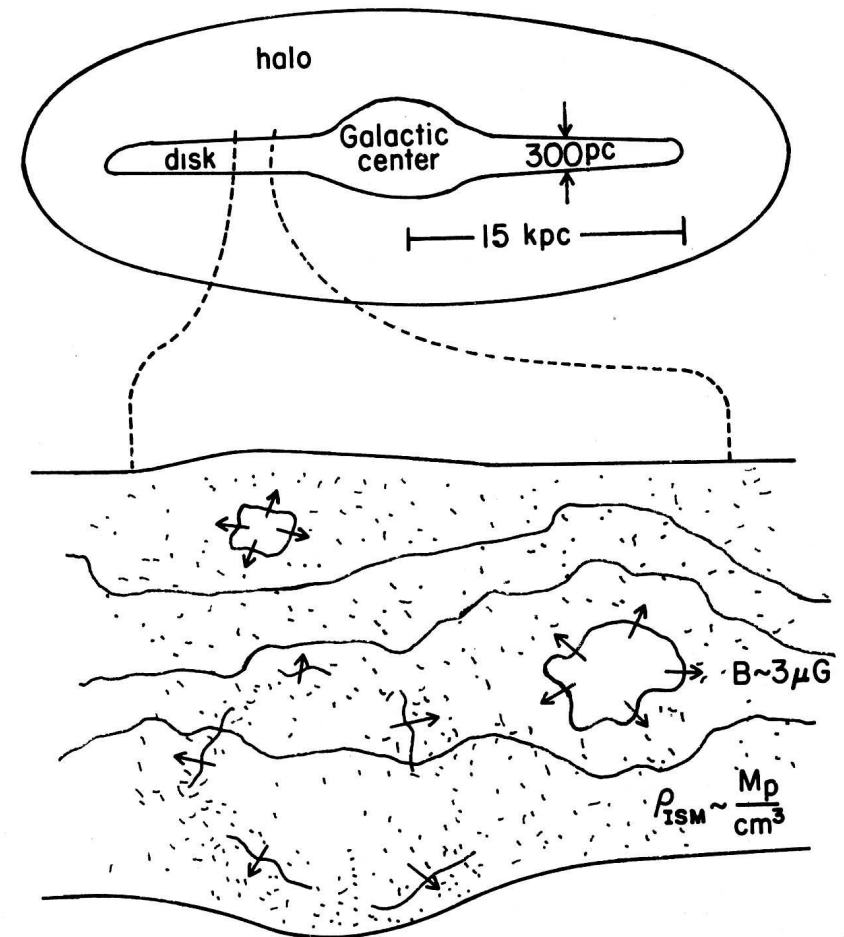


# Cosmic rays in the Galaxy

Propagation

119

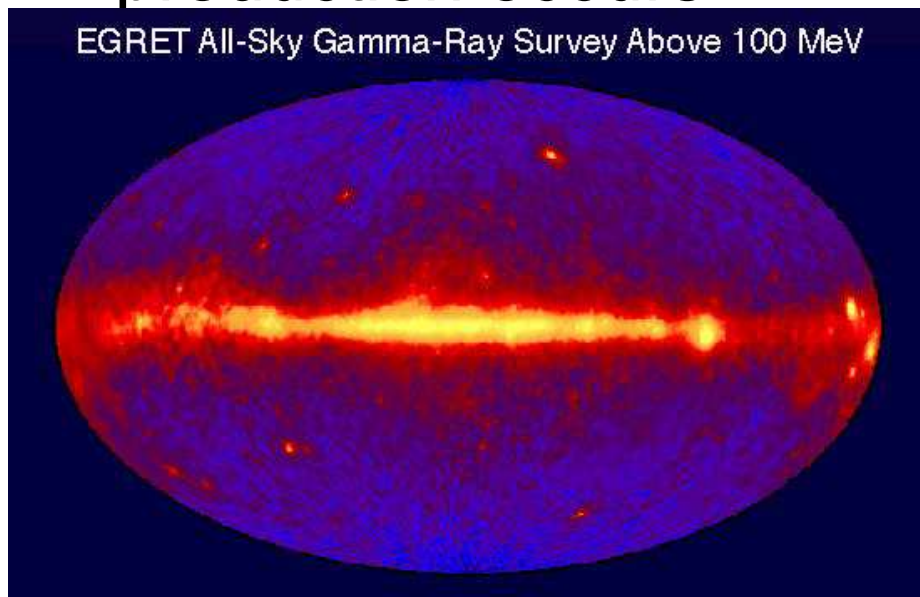
- Supernova explosions energize the ISM
  - ~1% Kinetic energy;  
neutrinos ~ 99%
  - >10% of kinetic energy → CR acceleration
  - Energy density in CR ~  $B^2/8\pi$
  - SN & CR activity drives Galactic wind into halo (Parker)
  - CR diffuse in larger volume
  - Eventually escape Galaxy



# Diffuse galactic secondaries

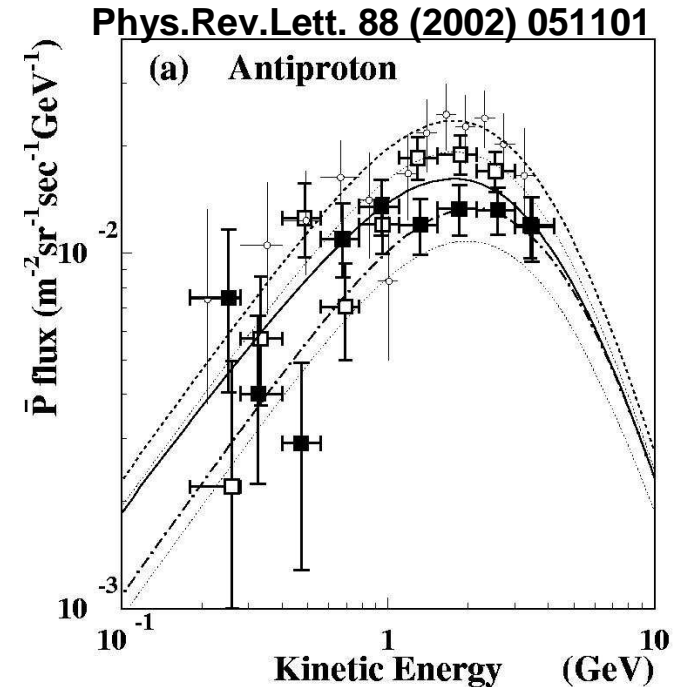
$p + \text{gas} \rightarrow \pi^0, \pi^{+/-},$   
antiprotons

- $\pi^0 \rightarrow \gamma\gamma$  [ $\pi^{+/-} \rightarrow \nu, \mu \rightarrow e^{+/-}$ ]
- $\gamma$ -spectrum depends on where production occurs



Berlin, 2009 29 Sept

Before Fermi & PAMELA



BESS antiprotons, 1997, '99, '00.  
• Fully consistent with secondary production by collisions in ISM followed by solar modulation varying with solar cycle

Tom Gaisser

27

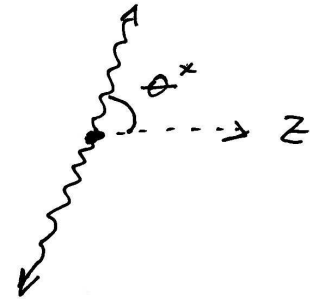
# Kinematics of $\pi^0$ decay

$\pi^0 \rightarrow \gamma \gamma$  decay in flight, direction = z axis

$$\frac{dN_\gamma}{d\Omega} = \frac{1}{2\pi} \frac{dN_\gamma}{d\cos\theta^*} = \text{constant}$$



In rest frame of  $\pi^0$



$$E_{\text{Lab}} = \gamma E^* + \beta \gamma p^* \cos\theta^*$$

$$p^* = E^* = \frac{m_{\pi^0}}{2} = 70 \text{ MeV}$$

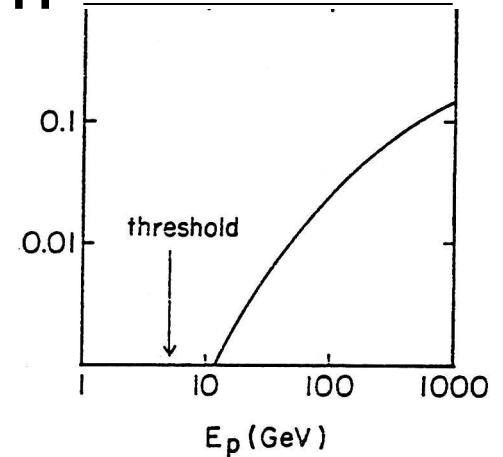
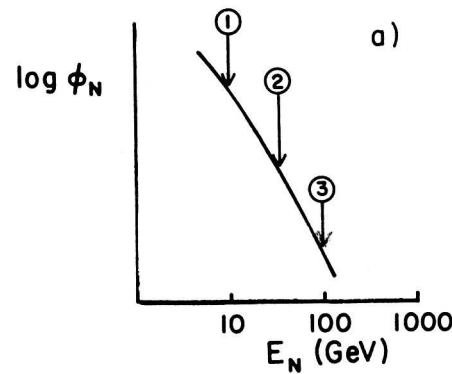
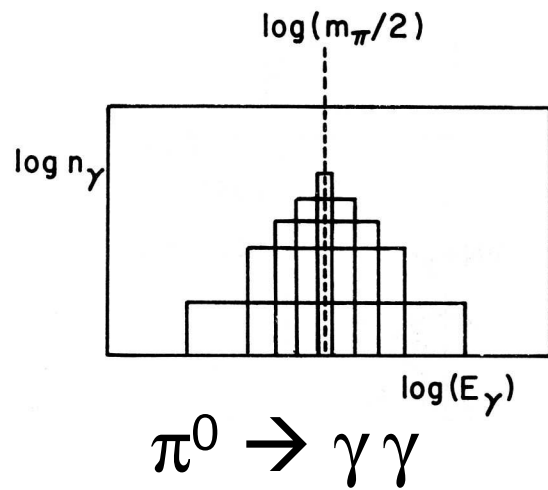
$$(1-\beta)\gamma \frac{m_\pi}{2} \leq E_{\text{Lab}} \leq (1+\beta)\gamma \frac{m_\pi}{2} \Rightarrow \frac{m_\pi}{2} \sqrt{\frac{1-\beta}{1+\beta}} \leq E_\gamma \leq \frac{m_\pi}{2} \sqrt{\frac{1+\beta}{1-\beta}}$$

Thus  $\ln \frac{m_\pi}{2} - \frac{1}{2} \ln \frac{1+\beta}{1-\beta} \leq \ln E_\gamma \leq \ln \frac{m_\pi}{2} + \frac{1}{2} \ln \frac{1+\beta}{1-\beta}$

E

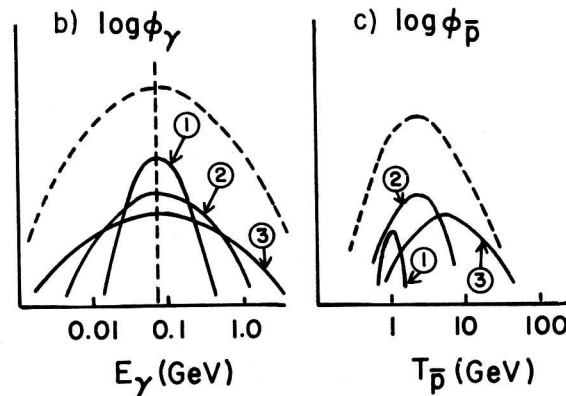
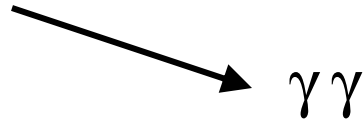
Flat distribution for fixed  $E_\pi$  with  $\langle \ln E_\gamma \rangle = \frac{m_\pi}{2}$

# Constructing secondary spectrum from primary spectrum



$\bar{p}$  per proton interaction

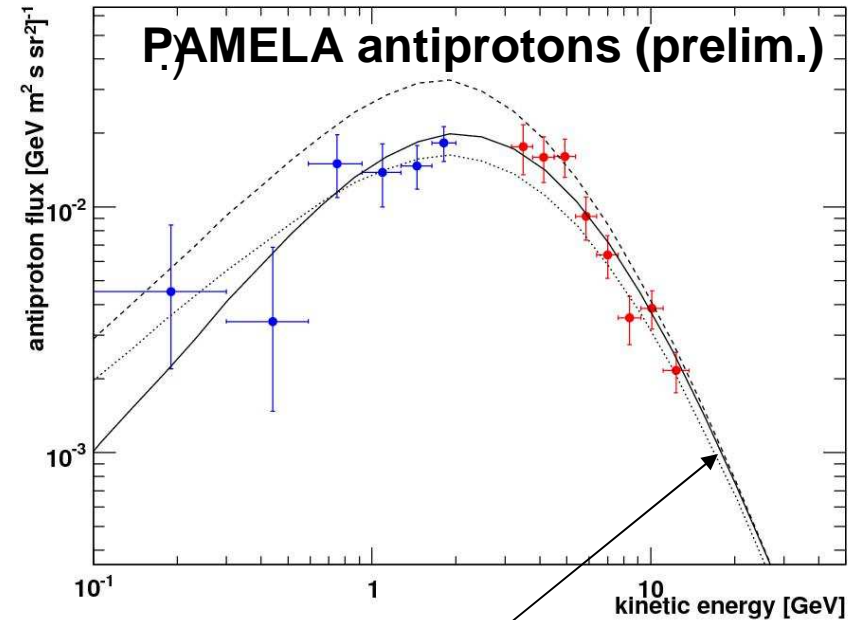
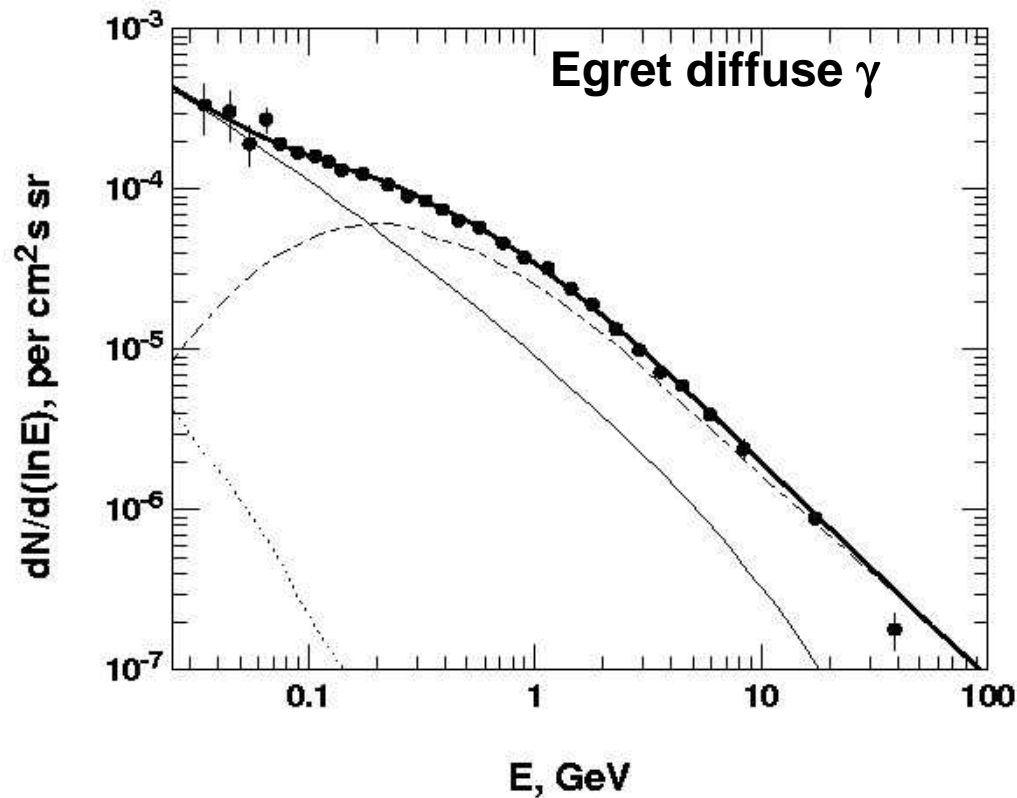
$p p \rightarrow \pi^0 + \text{anything}$



$p p \rightarrow \bar{p} + \text{anything}$

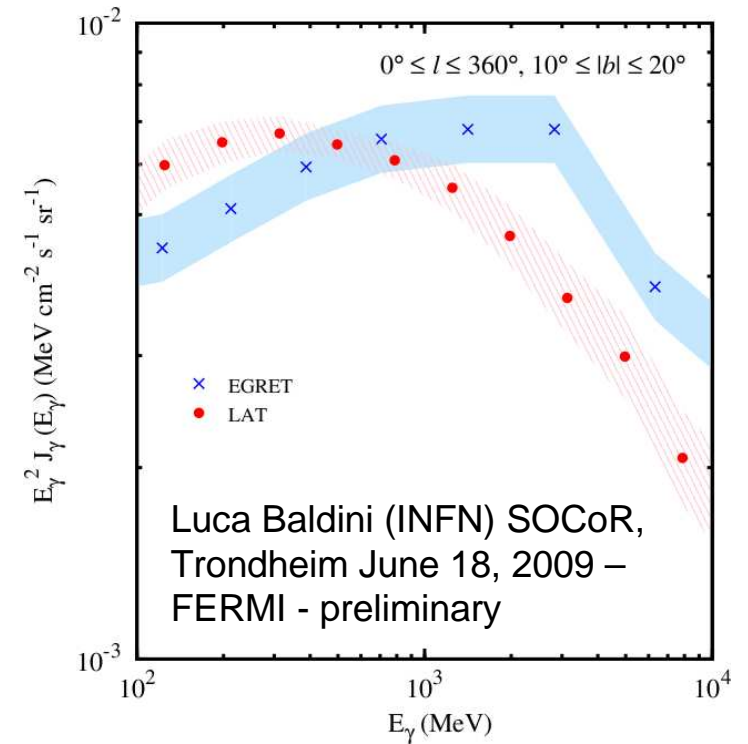
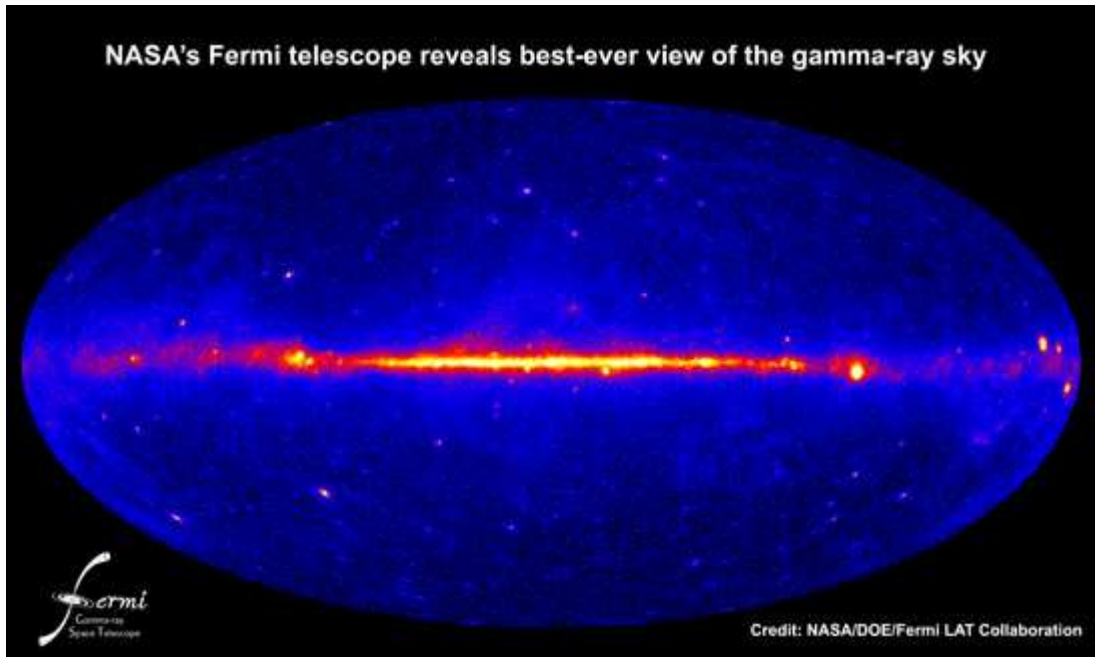
# Are all photons and $\bar{p}$ produced in ISM?

A fraction may be produced in the sources



**Secondary production:**  
**V. S. Ptuskin et al, ApJ**  
**642 (2006) 902**

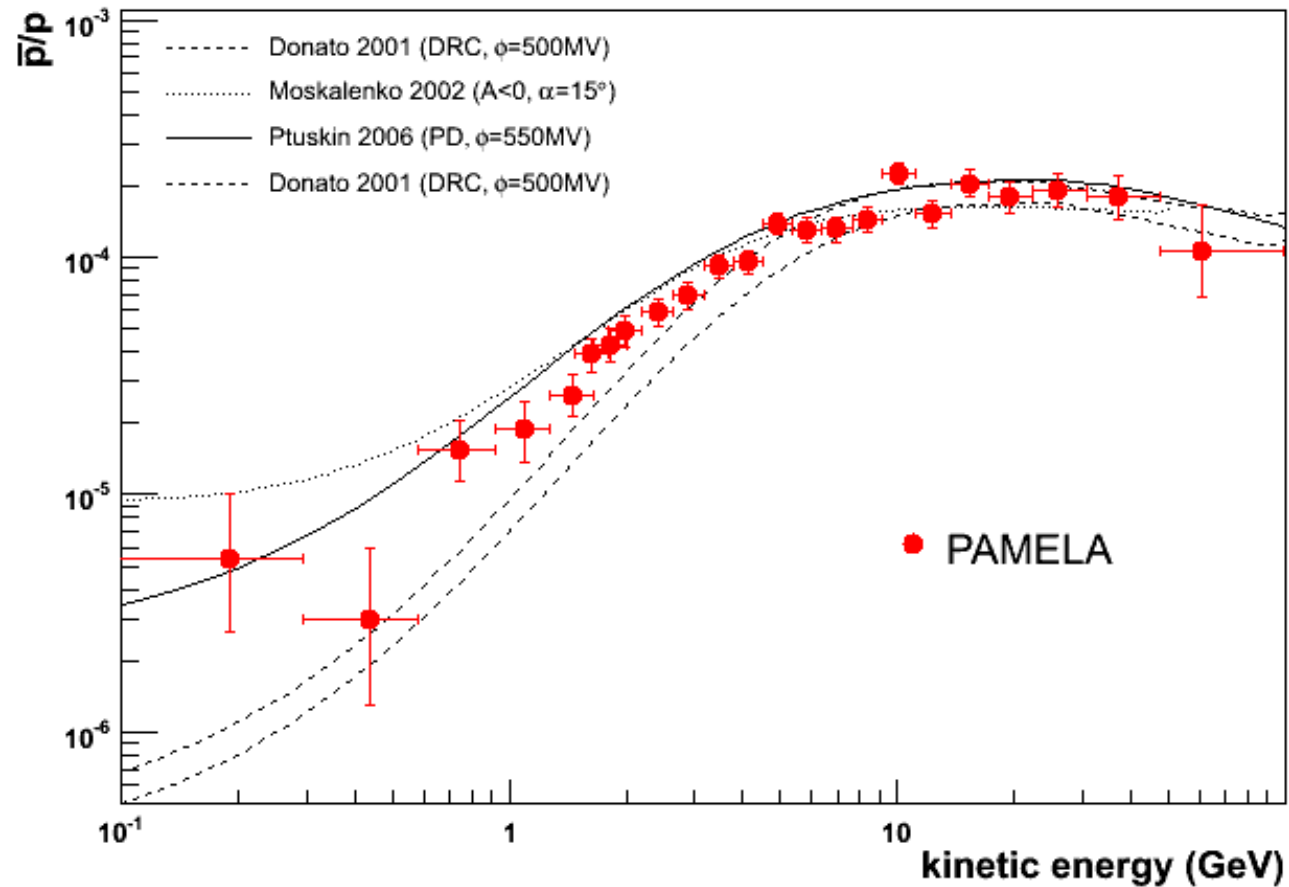
# Diffuse gamma-rays from FERMI



# Antiproton to proton ratio

PRL 102, 051101 (2009)

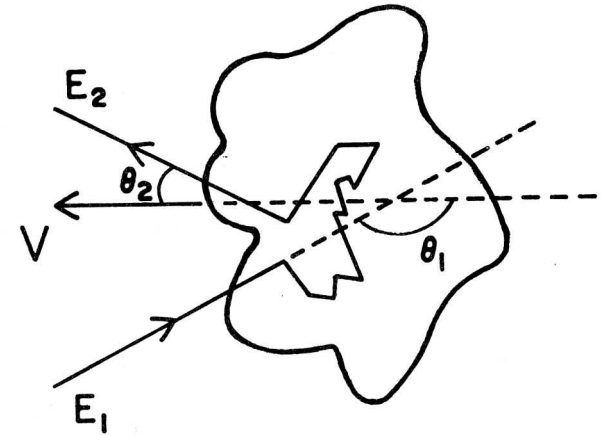
## Secondary Production Models



# Acceleration

Fermi acceleration mechanisms:

Transfer macroscopic energy of turbulent magnetized plasma to individual charged particles



Essential assumption:  $\Delta E = \xi E$

energy gain per encounter  $\propto$  Energy of particle.

After  $n$  encounters  $E_n = E_0 (1 + \xi)^n$

$P_{esc}$  = probability per cycle of particle being lost from acceleration region.

$n = \ln \frac{E}{E_0} / \ln (1 + \xi)$  needed to reach  $E$

Probability of surviving  $n$  cycles =  $(1 - P_{esc})^n$

$$N(\geq E) = \sum_{m=n}^{\infty} (1 - P_{esc})^m = \frac{(1 - P_{esc})^n}{P_{esc}}$$

$$\text{where } n = \ln \frac{E}{E_0} / \ln(1 + \xi)$$

$$N(\geq E) = \frac{1}{P_{esc}} \exp \left\{ \ln \frac{E}{E_0} \times \frac{\ln(1 - P_{esc})}{\ln(1 + \xi)} \right\}$$

$$= \frac{1}{P_{esc}} \left( \frac{E}{E_0} \right)^{-\gamma}, \quad \gamma = \frac{\ln \frac{1}{1 - P_{esc}}}{\ln(1 + \xi)} \sim \frac{P_{esc}}{\xi}$$

→  $\gamma =$  integral spectral index of power-law spectrum

$$P_{esc} \sim \frac{T_{cycle}}{T_{esc}} \quad (\text{from } \overset{\text{escape}}{\text{acceleration region}})$$

After a time  $t$ ,  $n_{max} = t / T_{cycle}$

$$\rightarrow \text{so } E \leq E_0 (1 + \xi)^{t / T_{cycle}}$$

"Scattering" = multiple bending in  
moving turbulent magnetic fields

= "collisionless" scattering

one "encounter" occurs when particle  
loses all memory of the direction with which  
it entered the scattering region

one cycle occurs when particle leaves  
the scattering region but is still available  
for another cycle of acceleration.

$$E_1' = \gamma E_1 (1 - \beta \cos \theta_1) \quad \text{after randomization inside scattering region}$$

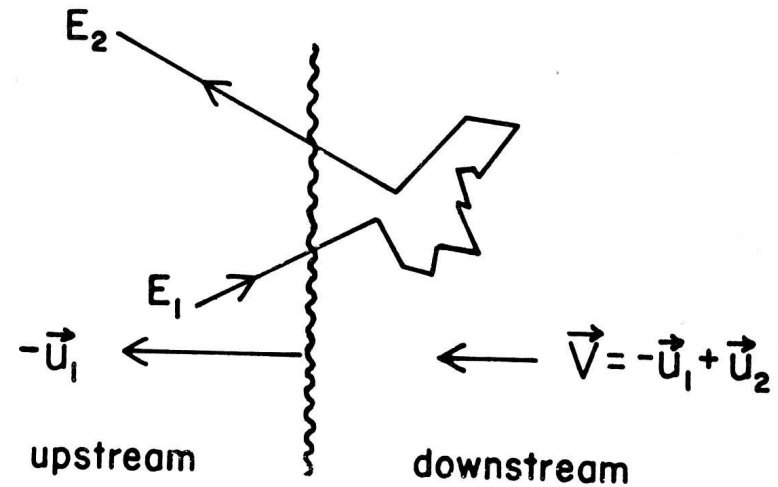
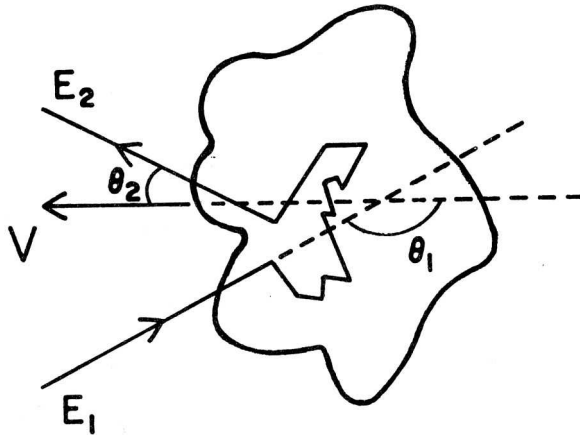
$$E_2' = E_1' \quad \text{because motion in magnetic field does not change energy}$$

$$E_2 = \gamma E_2' (1 + \beta \cos \theta_2)$$

$$\frac{E_2 - E_1}{E_1} = \frac{\Delta E}{E} = \frac{1 - \beta \cos \theta_1 + \beta \cos \theta_2 - \beta^2 \cos \theta_1 \cos \theta_2}{1 - \beta^2} - 1$$

Note:  $\Delta E$  for a single encounter may be + or - depending on  $\cos \theta_1$  or  $\cos \theta_2$

Next step is to average over  $\cos \theta_2$  and  $\cos \theta_1$



Distribution of exit angles ( $\cos \theta_2$ )

$$(a) \quad \frac{dn}{d \cos \theta'_2} = \text{constant}, \quad -1 \leq \cos \theta'_2 \leq 1,$$

$\cos \theta_2$  averages to 0 so

$$(a) \quad \frac{\langle \Delta E \rangle_2}{E_1} = \frac{1 - \beta \cos \theta_1}{1 - \beta^2} - 1$$

Distribution of entrance angles ( $\cos \theta_1$ ):

$$\frac{dn}{d \cos \theta_1} = \frac{c - V \cos \theta_1}{2c}, \quad -1 \leq \cos \theta_1 \leq 1,$$

$\cos \theta_1$  averages to  $-V/3c$  so

$$(a) \quad \xi = \frac{1 + \frac{1}{3}\beta^2}{1 - \beta^2} - 1 \sim \frac{4}{3}\beta^2$$

$$(b) \quad \frac{dn}{d \cos \theta'_2} = 2 \cos \theta'_2, \quad 0 \leq \cos \theta'_2 \leq 1.$$

$\cos \theta_2$  averages to  $2/3$  so that

$$(b) \quad \frac{\langle \Delta E \rangle_2}{E_1} = \frac{1 - \beta \cos \theta_1 + \frac{2}{3}\beta - \frac{2}{3}\beta^2 \cos \theta_1}{1 - \beta^2} - 1.$$

$-1 \leq \cos \theta_1 \leq 0$ , so that  $\langle \cos \theta_1 \rangle_b = -2/3$

then

$$(b) \quad \xi = \frac{1 + \frac{4}{3}\beta + \frac{4}{9}\beta^2}{1 - \beta^2} - 1 \sim \frac{4}{3}\beta = \frac{4}{3} \frac{u_1 - u_2}{c}.$$

Recall  $\gamma$  spectral index =  $P_{esc} / \Sigma = \frac{1}{\Sigma} \frac{T_{cyc}}{T_{esc}}$

For clouds (2nd order Fermi)  $T_{cyc} = \frac{1}{c \rho_c \sigma_c}$

$\rho_c$  = density of clouds

$\sigma_c$  = area of clouds

$c$  = velocity of cosmic ray

$T_{esc} \sim 7 \times 10^6$  yrs.

$\gamma = \frac{1}{\Sigma c \rho_c \sigma_c T_{esc}}$  is model dependent

For 1st order Fermi (large shock)

$$\#1 \text{ rate of encounters} = \int_0^1 d\omega \sin\theta \cos\theta \int_0^{2\pi} d\phi \frac{c \rho_{CR}}{4\pi} = \frac{c \rho_{CR}}{4}$$

$$\#2 \text{ rate of convection downstream} = \rho_{CR} u_2$$

$$\rho_{esc} = \frac{\#2}{\#1} = \frac{\rho_{CR} u_2}{c \rho_{CR} / 4} = \frac{4 u_2}{c}$$

$$\gamma = \frac{\rho_{esc}}{\xi} = \frac{4 u_2}{c} \times \frac{3}{4} \frac{c}{u_1 - u_2} = \frac{3}{u_1/u_2 - 1}$$

From kinetic theory of gas  $\frac{u_1}{u_2} = \frac{\rho_2}{\rho_1} = \frac{(\frac{5}{3} + 1) M^2}{(\frac{5}{3} - 1) M^2 + 2}$

$M$  = Mach number,  $\frac{5}{3} = \frac{c_p}{c_v}$

$\frac{u_1}{u_2} \rightarrow 4$  for strong shocks and  $\gamma \rightarrow 1$

$$\frac{dE}{dt} = \frac{\sum E}{T_{\text{cycle}}} = \text{acceleration rate}$$

Diffusion coefficient  $D = \frac{1}{3} \lambda c$

$$T_{\text{cycle}} \sim \frac{\lambda}{u_1} \geq \frac{r_L}{u_1} = \frac{E}{u_1 z e B}$$

$$\frac{dE}{dt} \sim \sum u_1 z e B = \frac{4}{3} \frac{u_1 - u_2}{c} u_1 z e B$$

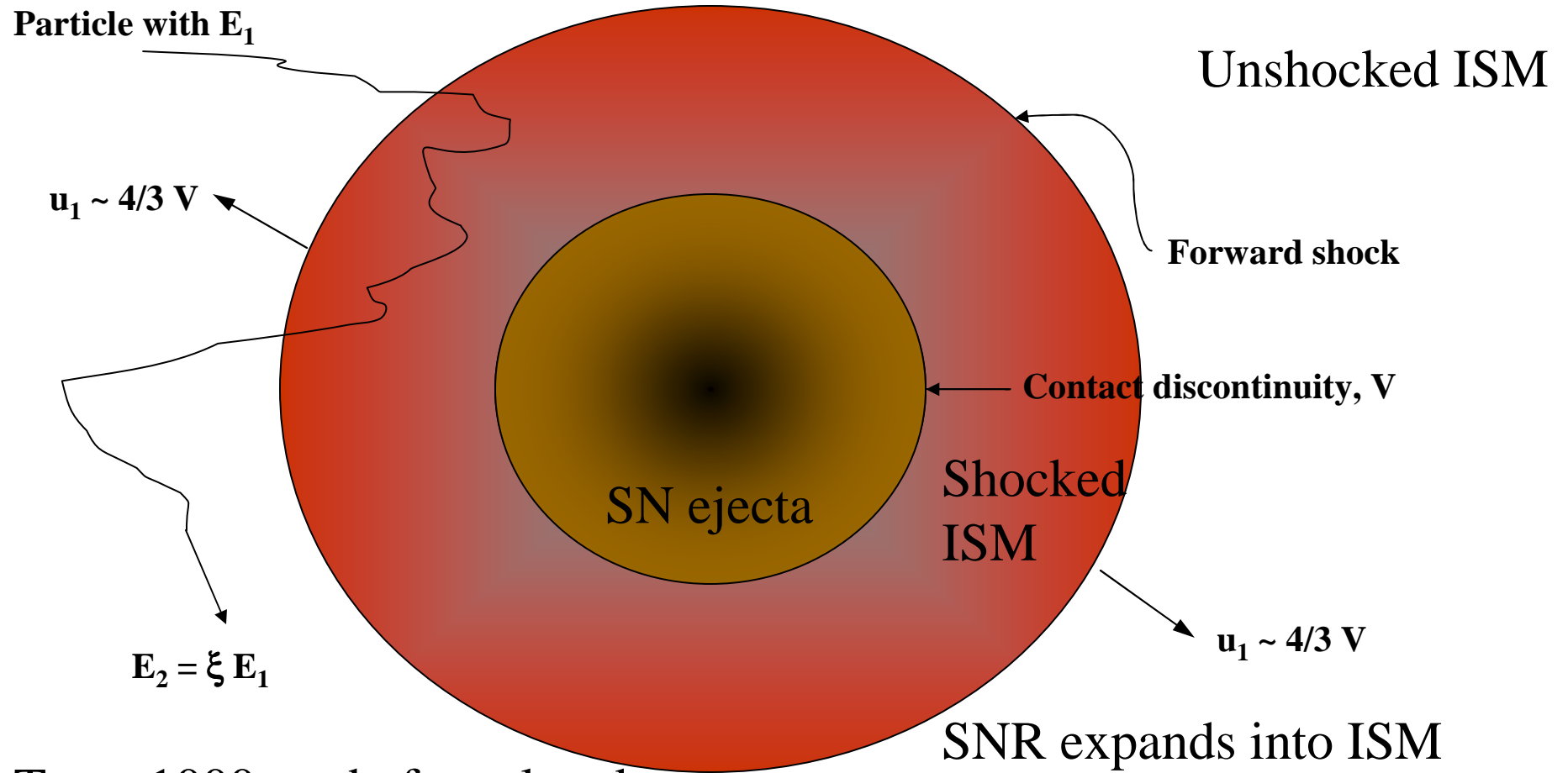
in time T

$$E_{\text{max}}(T) \sim \frac{4}{3} \frac{3}{4} \frac{u_1^2}{c} z e B T \quad \text{or } u_1^4$$

$$\frac{4}{3} \pi (u_1 T)^3 \rho_{\text{ISM}} = M_{\text{ejecta}} \sim \underbrace{2 \times 10^{34}}_{10 M_{\odot}} \text{ g} \Rightarrow T \sim 1500 \text{ yrs}$$

$$E_{\text{max}} \sim 100 \text{ TeV}$$

# Supernova blast wave acceleration



$T_{SN} \sim 1000$  yrs before slowdown

$E_{max} \sim Z \times 100$  TeV

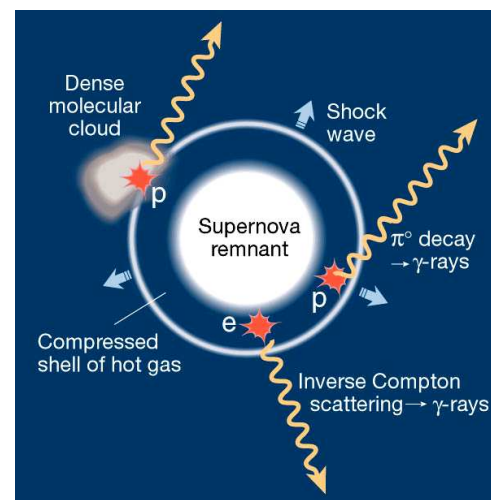
Berlin, 2009 29 Sept

Tom Gaisser

SNR expands into ISM  
with velocity  $V \sim 10^4$  km/s.  
Drives forward shock at  $4/3 V$

# Problems of simplest SNR shock model

- Expected shape of spectrum:
  - Differential index  $\alpha \sim 2.1$  for diffusive shock acceleration
    - $\alpha_{\text{observed}} \sim 2.7$ ;  $\alpha_{\text{source}} \sim 2.1$ ;  
 $\Delta\alpha \sim 0.6 \rightarrow \tau_{\text{esc}}(E) \sim E^{-0.6}$
    - $c \tau_{\text{esc}} \rightarrow T_{\text{disk}} \sim 100 \text{ TeV}$
    - $\rightarrow$  Isotropy problem
- $E_{\text{max}} \sim \beta_{\text{shock}} Z e \times B \times R_{\text{shock}}$ 
  - $\rightarrow E_{\text{max}} \sim Z \times 100 \text{ TeV}$  with exponential cutoff of each component
  - But spectrum continues to higher energy:
    - $\rightarrow E_{\text{max}}$  problem
- Expect  $p + \text{gas} \rightarrow \gamma$  (TeV) for certain SNR
  - Need nearby target as shown in picture from *Nature* (F. Aharonian, April 02)
  - Some likely candidates (e.g. HESS J1745-290) but still no certain example
  - $\rightarrow$  Problem of elusive  $\pi^0$   $\gamma$ -rays



# Solutions to problems ?

- Isotropy problem
  - $\gamma_{\text{source}} \sim 2.3$  and  $\tau_{\text{esc}} \sim E^{-0.33}$  ??
  - $\tau_{\text{esc}} \sim E^{-0.33}$  is theoretically preferred, but  $\gamma = 2.3$ ?
- Evidence for acceleration of protons at SNR
  - Look for TeV  $\gamma$ -rays mapping gas clouds at SNR
  - Possible example SNR IC443 (VERITAS, arXiv:0810.0799)
- Acceleration to higher energy
  - Magnetic field amplification in non-linear shock acceleration

# Non-linear shock acceleration

- Discussion of acceleration so far
  - “Test particle” approximation
  - Neglects effects of particles being accelerated on the accelerator
- Non-linear theory
  - Accounts for magneto-hydrodynamic turbulence generated by cosmic-rays upstream of the shock.
  - Cosmic-rays scatter on MHD turbulence with wavelength matched to particle’s gyro-radius
- Two important effects
  - Spectrum is distorted
  - Magnetic field in acceleration region is amplified

# Non-linear shock acceleration - 2

- Cosmic-ray pressure in upstream region generates precursor
- Higher energy particles get further upstream
- Experience larger discontinuity  $r = u_1(x) / u_2$

$$\frac{dN}{d \ln E} \sim E^{-\gamma}, \quad \gamma = \frac{3}{r-1} \quad \text{where } r = \frac{u_1}{u_2}$$

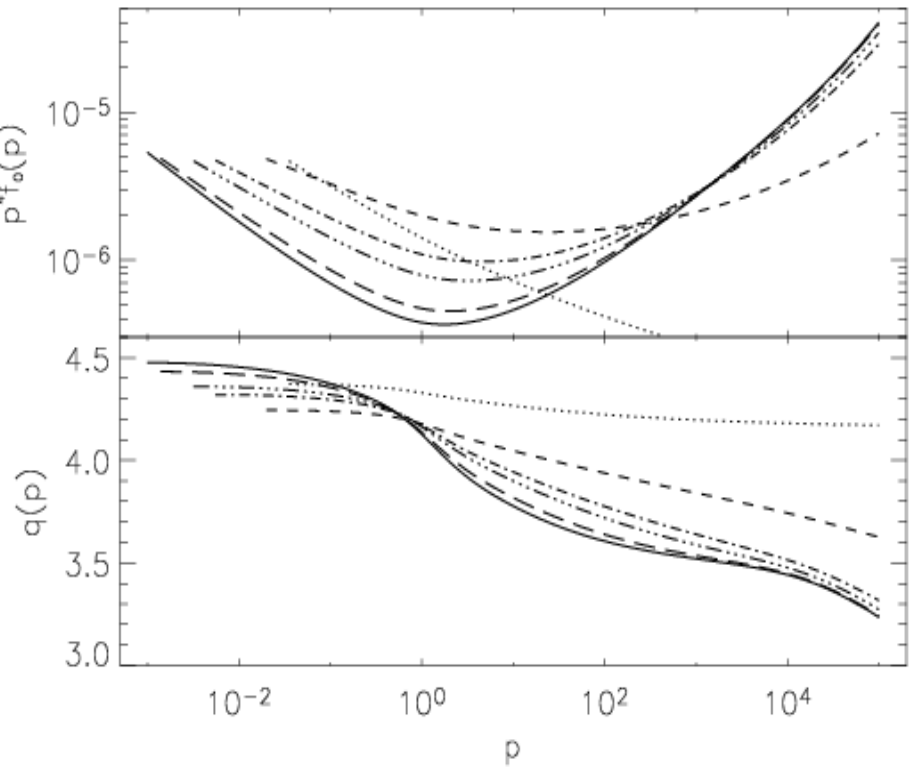
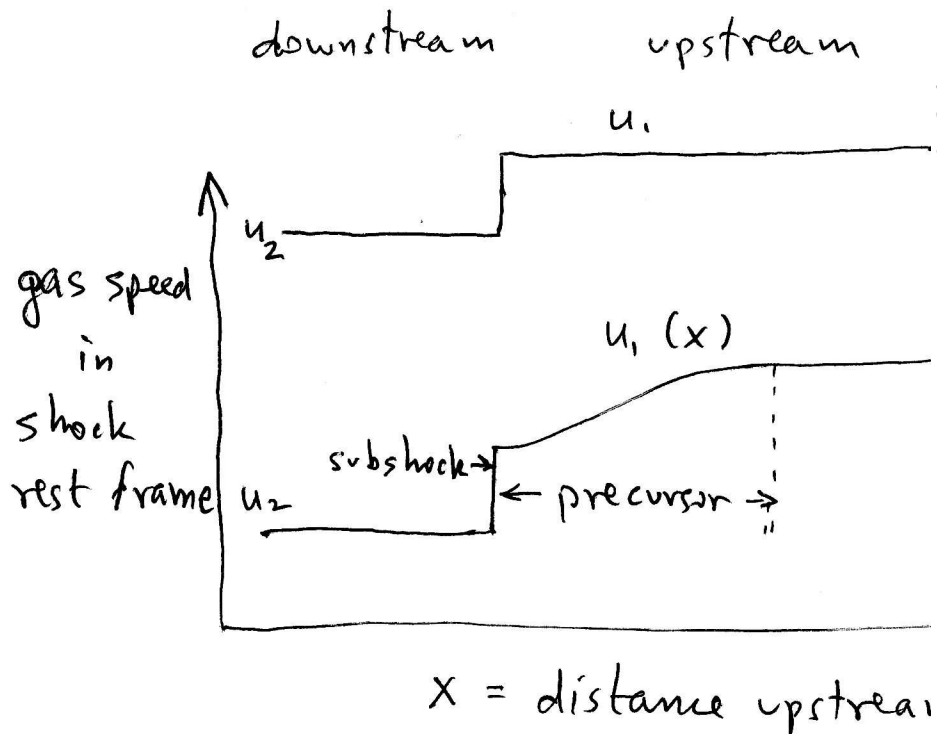
$$r = 4 - \frac{12}{(\text{Mach})^2} \quad \text{at subshock}$$

$$\Rightarrow \gamma = 1 + \epsilon \quad \text{at subshock}$$

$r > 4$  upstream of CRMS

$$\text{Example: } r = 7 \Rightarrow \gamma = \frac{1}{2}$$

# Non-linear shock acceleration - 3



- Spectrum at shock concave,
- $\gamma < 1$  at high energy,
- energy concentrated at  $E_{\max}$

Note: CR acceleration theory calculates distribution in  $p$ -space:  
 $f(p) \equiv dn_{\text{cr}} / dp^3 \sim (1/p^2) dn/dE$   
 So here  $q = \gamma + 3$

# Non-linear shock acceleration - 4

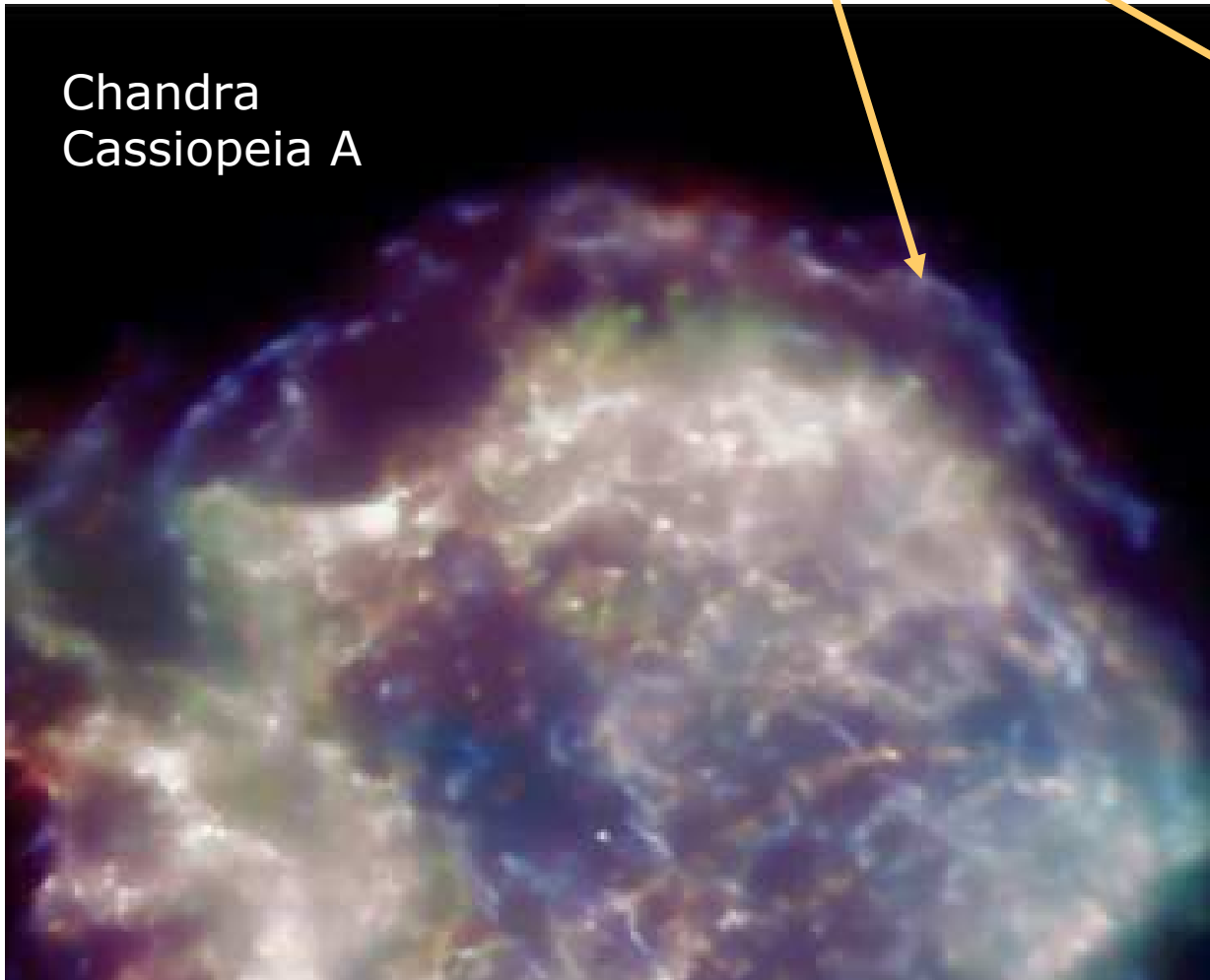
- Cosmic-ray pressure also amplifies magnetic field (Bell, MNRAS 353, 550, 2004)
- $E_{\max}$  increases to  $10^{16}$  or  $10^{17}$  eV in early, free-expansion phase of SNR expansion
- applies to small fraction of accelerated particles

ALSO (Ptuskin & Zirakashvili, A&A 429, 755, 2005 )

- In later phases of SNR expansion:
  - upstream scattering becomes inefficient as expansion slows down
  - $E_{\max} \rightarrow E_{\max}(t)$  decreases with time
  - Accelerated particles with  $E > E_{\max}(t)$  escape upstream
  - observed spectrum is integral of SNR history

Filamentary structure of X-ray emission  
of young SNRs:  
Evidence for amplification  $B \sim 100 \mu\text{G}$

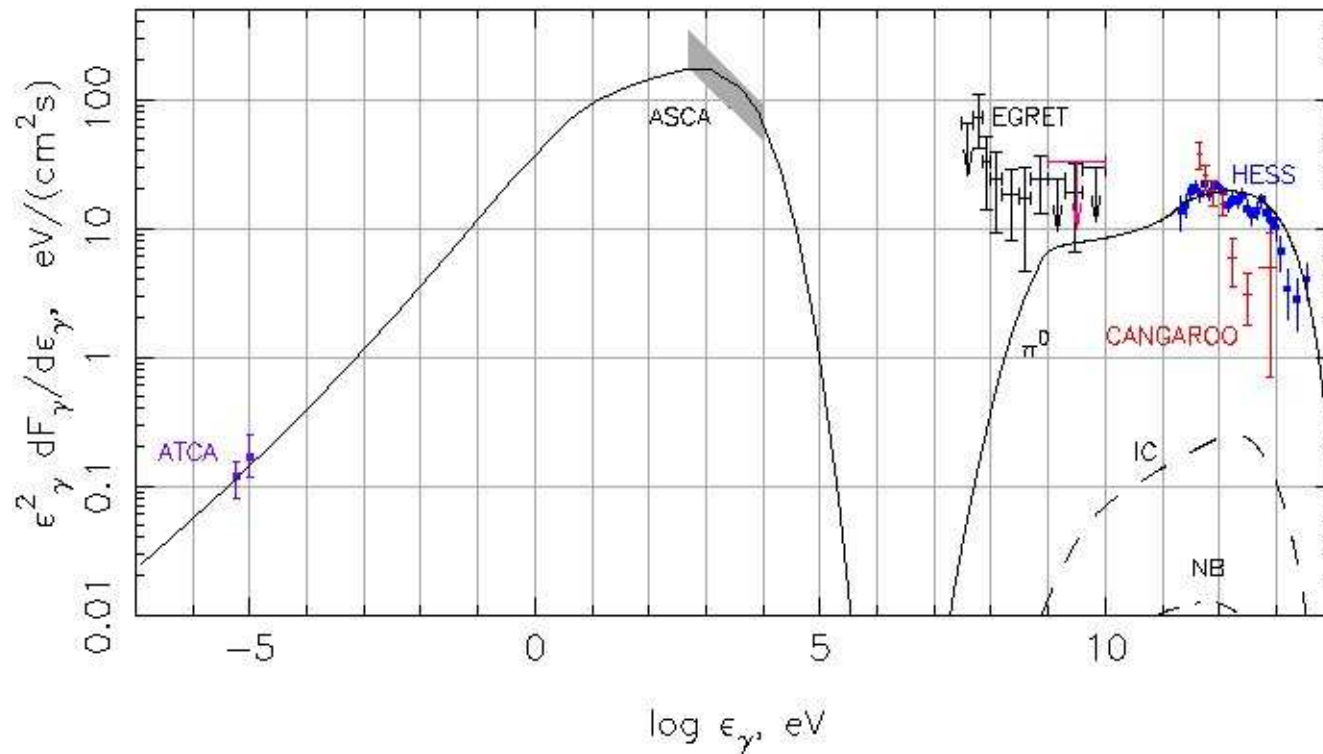
Berezhko&Volk, OG111



# RX J1713.7-3946

Berezhko & Völk, arXiv:0707.4647

**Contributions from electrons (IC, NB) suppressed by  $\sim 100 \mu\text{G}$  fields**



# Examples of power-law distributions

(M.E.J. Newman, cond-mat/0412004)

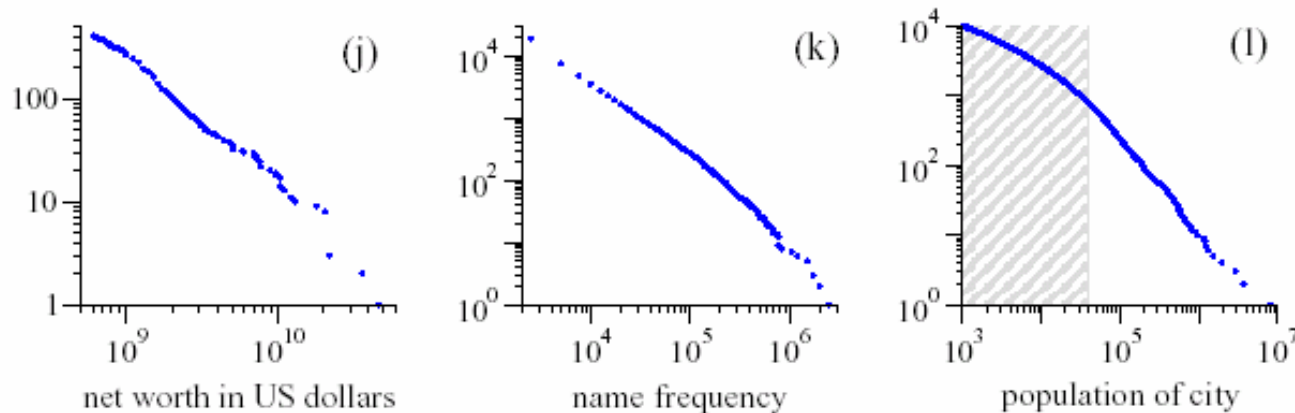
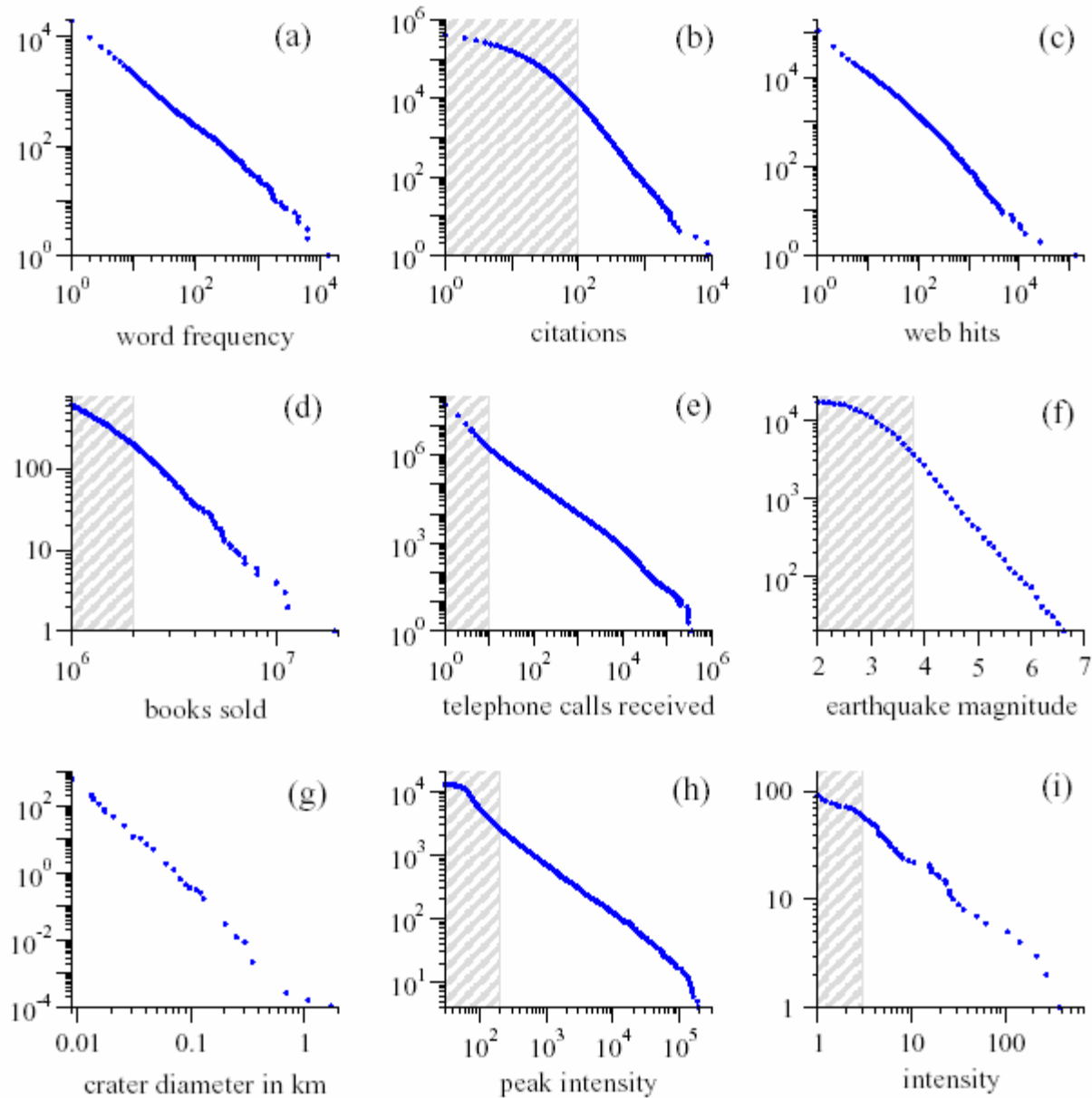


FIG. 4 Cumulative distributions or “rank/frequency plots” of twelve quantities reputed to follow power laws. The distributions were computed as described in Appendix A. Data in the shaded regions were excluded from the calculations of the exponents in Table I. Source references for the data are given in the text. (a) Numbers of occurrences of words in the novel *Moby Dick* by Hermann Melville. (b) Numbers of citations to scientific papers published in 1981, from time of publication until June 1997. (c) Numbers of hits on web sites by 60 000 users of the America Online Internet service for the day of 1 December 1997. (d) Numbers of copies of bestselling books sold in the US between 1895 and 1965. (e) Number of calls received by AT&T telephone customers in the US for a single day. (f) Magnitude of earthquakes in California between January 1910 and May 1992. Magnitude is proportional to the logarithm of the maximum amplitude of the earthquake, and hence the distribution obeys a power law even though the horizontal axis is linear. (g) Diameter of craters on the moon. Vertical axis is measured per square kilometre. (h) Peak gamma-ray intensity of solar flares in counts per second, measured from Earth orbit between February 1980 and November 1989. (i) Intensity of wars from 1816 to 1980, measured as battle deaths per 10 000 of the population of the participating countries. (j) Aggregate net worth in dollars of the richest individuals in the US in October 2003. (k) Frequency of occurrence of family names in the US in the year 1990. (l) Populations of US cities in the year 2000.

# More examples from M.E.J. Newman, cond-mat/0412004



Berlin, 2009

# Casualties per attack in Iraq

(Neil F. Johnson, et al., from *APS News*, 8 Nov 2006)

## The Mother (Nature) of All Wars?

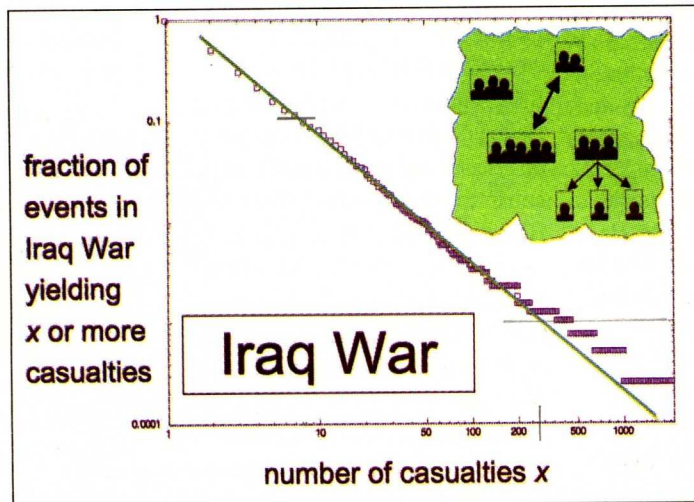
### Modern Wars, Global Terrorism, and Complexity Science

by Neil F. Johnson

sia.” We are then typ-  
tudio experts who try  
awing on idiosyncrat-  
Although often uncon-  
/ defensible given the  
ocations and durations  
r recent research by a  
ity scientists suggests  
l and strategic experts  
il.

s of Complex Systems,  
he dynamics underly-  
iding global terrorism,  
nore they have devel-  
ibing the dynamics of  
attacks, which neatly  
served in all modern  
ms are quite sobering:  
ms of modern conflicts,  
e are operating in the  
the same enemy on all

field of human conflict  
irst, the increased avail-  
eans that there is a data  
ocial sciences—just as  
might alight as a result



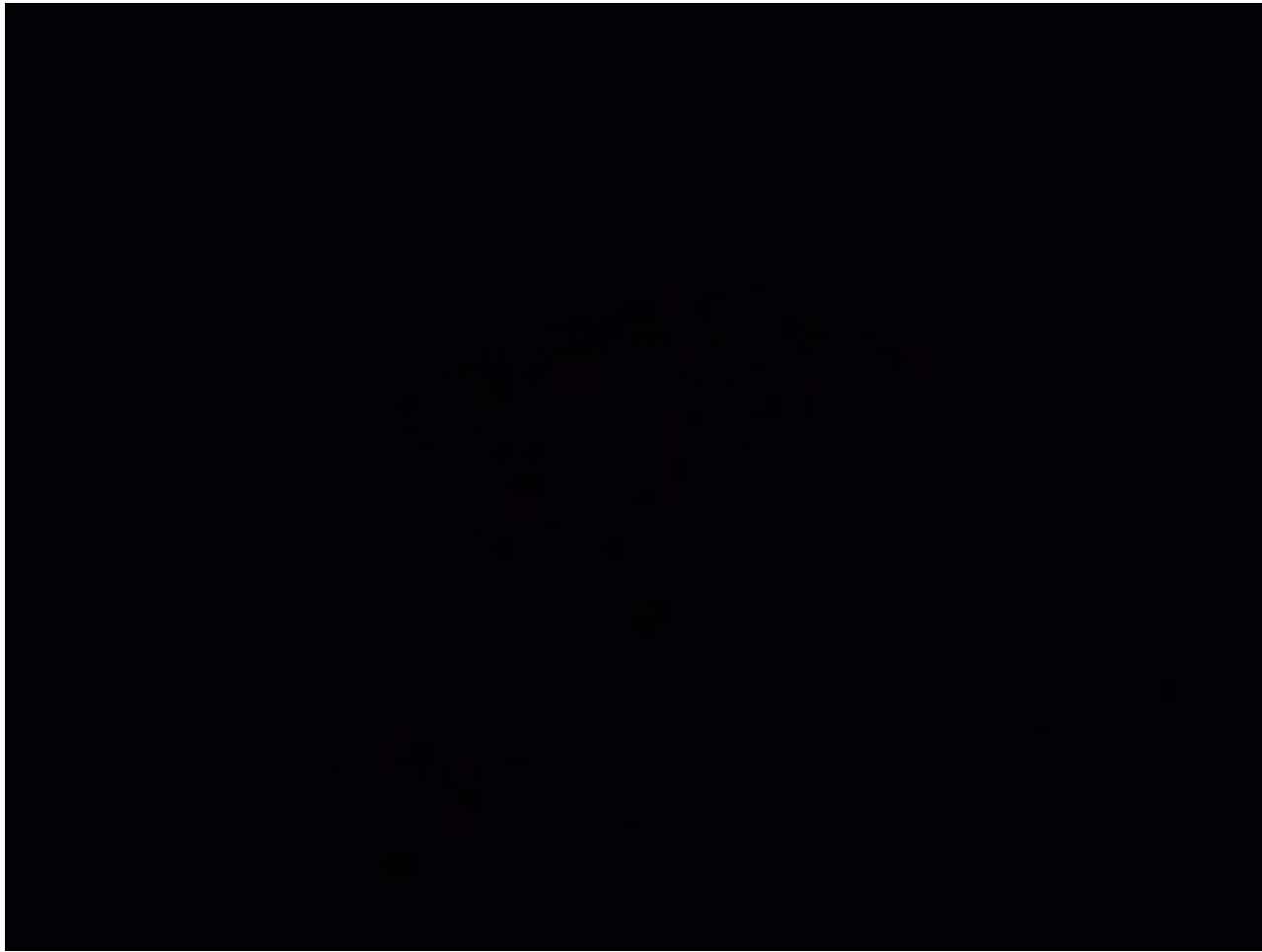
Log-log plot of the fraction of all events in the Iraq War with  $x$  or more casualties, versus  $x$ . Squares are actual war data. The line is produced by the physics-based analytic model (see inset). All modern wars, including terrorism, show power-law like behavior with exponents in the vicinity of 2.5. The analytic model considers insurgent armies as an ecology of attack units, which undergo frequent coalescence and fragmentation. The number of dark shadows is proportional to the number of casualties which each attack unit can typically inflict in a conflict event. Full details are given in e-print “Universal patterns underlying ongoing wars and terrorism,” by Neil F. Johnson, Mike Spagat, Jorge A. Restrepo, Oscar Becerra, Juan Camilo Bohorquez, Nicolas Suarez, Elvira Maria Restrepo, Roberto Zarama, which is available at <http://xxx.lanl.gov/abs/physics/0605035>

When our mod-  
power-law with  $\alpha$   
ation-dissociati-  
group sizes, this  $\alpha$   
thereby incorpora  
Generalizing the r  
gent groups, yields  
the entire range of  
at high and low  $x$ .  
of casualty events  
slight variations c

While outside t  
line of physics re  
understanding of  
insurgent warfare.  
ics of insurgent g  
arenas—from the  
deserts of Iraq, anc  
al terrorism. In sh  
terrorism are beir  
or ideology, and r  
ics of human insu  
way in which insu  
faced with a mucl  
a consequence c  
stronger, but mor  
the same statistic

Differential  
 $\alpha \sim 2.5$

Berlin,



# Frank Capra, 1957